Article

Not peer-reviewed version

Controls on the Transformation of Clay Minerals in the Miocene Evaporite Deposits of the Ukrainian Carpathian Foredeep: An Overview

Yaroslava Yaremchuk , Sofiya Hryniv , Tadeusz Peryt *

Posted Date: 21 February 2025

doi: 10.20944/preprints202502.1716.v1

Keywords: clay minerals; marine evaporites; brines; Miocene; caprock; X-ray diffraction

 doi:10.20944/preprints202502.1716.v1

Article

Controls on the Transformation of Clay Minerals in the Miocene Evaporite Deposits of the Ukrainian Carpathian Foredeep: An Overview

Yaroslava Yaremchuk [1], Sofiya Hryniv [1] and Tadeusz Peryt [2,*]

[1] Institute of Geology and Geochemistry of Combustible Minerals of National Academy of Sciences of Ukraine, Naukova 3a, 79060 Lviv, Ukraine

[2] Polish Geological Institute – National Research Institute, Rakowiecka 4, 00-975 Warszawa, Poland

* Correspondence: tadeusz.peryt@pgi.gov.pl

Abstract: Clays deposited in marine evaporite sequences are strongly altered and the most important factor determining their transformation is the brine concentration. X-ray diffraction study of clay minerals associated with the Lower and Middle Miocene evaporite formations of the Ukrainian Carpathian Foredeep indicated that the clay mineral associations in the gypsum facies are composed of smectite and illite, and in some samples mixed-layer chlorite-smectite and illite-smectite as well as chlorite. In the halite facies, illite, chlorite and mixed-layer illite-smectite occur in rock salt of Eggenburgian age (Vorotyshcha Suite); in addition to those minerals, smectite, corrensite and mixed-layer chlorite-smectite occur in the Badenian rock salt (Tyras Suite); and in the potash facies illite and chlorite were recorded. Such clay mineral associations resulted from aggradational transformation of unstable and labile minerals and phases (kaolinite, smectite and mixed-layer phases) that finally pass into illite and chlorite: minerals that are stable in an evaporite environment. In addition to brine concentration control, another important factor in the transformations of clay minerals was sorption of organic components on the mineral structure, that slows the transformation processes. The association of clay minerals in the weathering zone of the evaporite deposits, besides inherited illite and chlorite, contains also mixed-layer illite-smectite and kaolinite. The appearance of those clay minerals in hypergene deposits is the consequence of two processes: degradational transformation (illite-smectite) and neoformation (kaolinite) in conditions of decreased ionic concentrations during desalination.

Keywords: clay minerals; marine evaporites; brines; Miocene; caprock; X-ray diffraction

1. Introduction

The origin of clay minerals in various geological environments (weathering, sedimentary, and diagenetic-hydrothermal) are provided by three mechanisms of clay mineral formation: inheritance, neoformation, and transformation [1,2].

One of these, transformation, has exceptional importance in the forming of clay mineral associations. The concept of transformation was introduced by [3] and includes degradation (negative transformation related to weathering and removal of matter) and aggradation (positive transformation related to growth of the crystalline structure and incorporation of matter) [3]. Transformations of clay minerals by degradation are common in the soil-forming process, where leaching is intense. Aggradational transformations are characteristic of the depositional environment, where ions from concentrated solutions can participate in the building of well-structured lattices. Illite and chlorite are typical of the premetamorphic stage of aggradation, the mixed-layer minerals represent intermediate stages of the processes of degradation and aggradation [4,5].

One of main transformation factors of clay minerals in different geological contexts is burial diagenesis of clay-rich deposits, for example, illitization of smectite ([6] and references therein). In

 doi:10.20944/preprints202502.1716.v1

evaporative conditions the most important factor in the transformation of clay minerals is the brine concentration [7,8].

Clay minerals of evaporite deposits are mostly regarded as authigenic [1,7,9–12]. Transformation or neoformation of clay minerals at the stage of sedimentation in an evaporite basin or at the stage of diagenesis within evaporite deposits are controlled by physico-chemical conditions and in a hypersaline environment this depends on such factors as temperature [13], lateral salinity change and alkalinity [14], and salinity combined with higher burial-related temperatures [15,16].

Associations of clay minerals of the Lower and Middle Miocene evaporites of the Carpathian region are well studied (see [17], for a review). Considerable attention has been paid to transformation processes of clay minerals under the influence of brines in salt basins or buried within deposits. Being unstable in conditions of increased salinity, allogenic minerals (kaolinite, smectite and mixed-layer phases) are transformed, through a series of transitional phases, into illite and chlorite [5,18]. As brine concentration increases further, the structure of those end-minerals becomes better ordered. Less attention has been paid to degradational transformation processes of clay minerals of the Miocene evaporites, that formed as brine concentrations decreased under the influence of surface waters. The mechanism of these transformations is related to destabilization of interlayer intervals of clay structures and the formation of labile phases.

The present research considers factors controlling the transformational processes of clay minerals in Miocene evaporite deposits of the Ukrainian Carpathian Foredeep.

1.1. Geological Setting

The Miocene Carpathian Foredeep is asymmetrical and developed as a peripheral foreland basin related to the moving Carpathian front [19]. The molasse, predominantly siliciclastic, deposits are up to 6 km thick in the Ukrainian Carpathian Foredeep where three tectonic zones are distinguished: outer (Bilche-Volytsya Zone), central (Sambir Nappe thrusted over the Bilche-Volytsya Zone) and inner (Boryslav-Pokuttya Nappe thrusted over the Sambir Nappe) [19,20] (Figures 1 and 2).

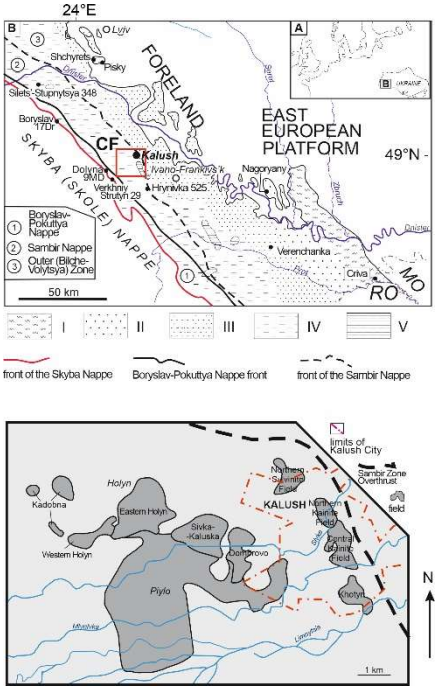

Figure 1. A, B: Location of sample sites; tectonic zonation of the Carpathian Foredeep after [21]; CF – Carpathian Foredeep; MO – Moldova; RO – Romania; I–V – evaporite facies zones of the Tyras Suite for the Outer (Bilche-Volytsya) Zone and below the Sambir and Boryslav-Pokuttya nappes (after [22]): I-IV indicate gypsum facies (in the case of IV, gypsum and/or anhydrite facies), V – halite facies; the red box indicates the area of the Kalush-

 doi:10.20944/preprints202502.1716.v1

Holyn potash deposit with the distribution of exploited areas (after [23], simplified) shown in the lower part of the figure.

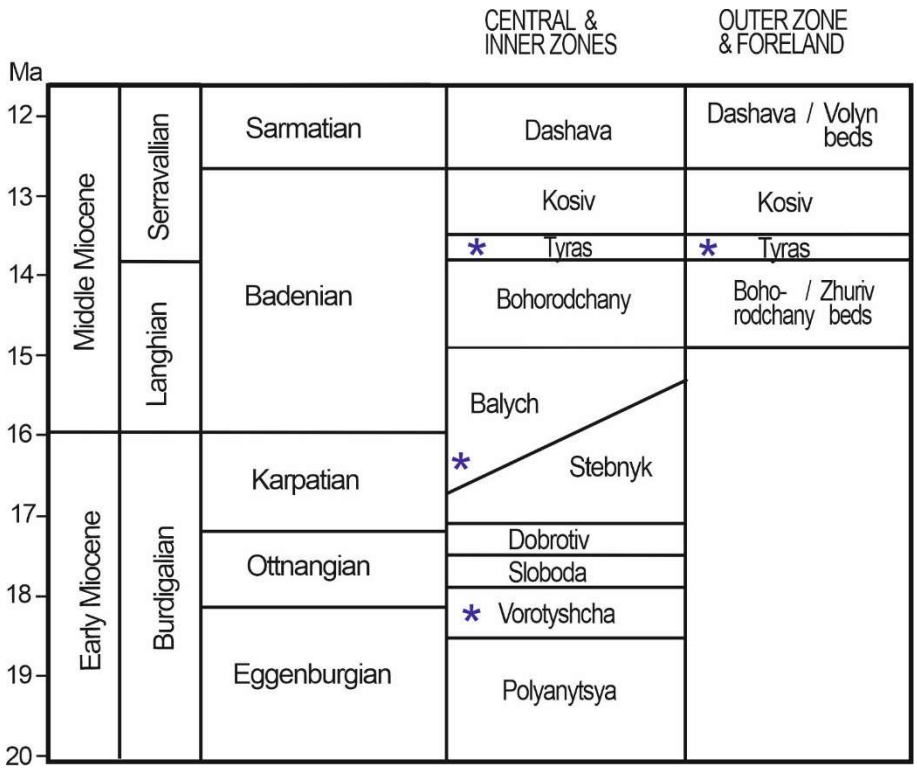

Figure 2. Regional stratigraphic scheme of Miocene strata in the Ukrainian Carpathian Foredeep (after [19], based on [19,24–26]). Note that the boundaries of formations are strongly diachronous according to [25] but this is here visualized only in the case of the boundary between the Stebnyk and Balych formations. The Miocene time scale is partly recalibrated and correlated to regional stages of the Central Paratethys (after [27]).

Evaporite deposits occurring in the Carpathian Foredeep fill (Figure 2) are involved in the thrusting of the Carpathian nappes and thus their stratigraphic sections are likely multiplied [28–31]. For example, the Lower Miocene (Eggenburgian) Vorotyshcha Suite of the inner zone shows a total thickness more than 2000 m [32], but the primary section was 100–125 m thick (Figure 3; [31]). The stratigraphic position of another potash deposit recorded higher in the stratigraphic section, the Kalush-Holyn deposit, is controversial (see [33], with references therein). A recent map synthesis [34] and the officially-approved stratigraphical scheme [23] consider that the Kalush-Holyn deposit is related to the upper part of the Balych Suite of Karpatian age, and [35,36] correlate “the Kalush Beds” with the Upper Badenian salt of the Wieliczka and Bochnia region (Poland).

 doi:10.20944/preprints202502.1716.v1

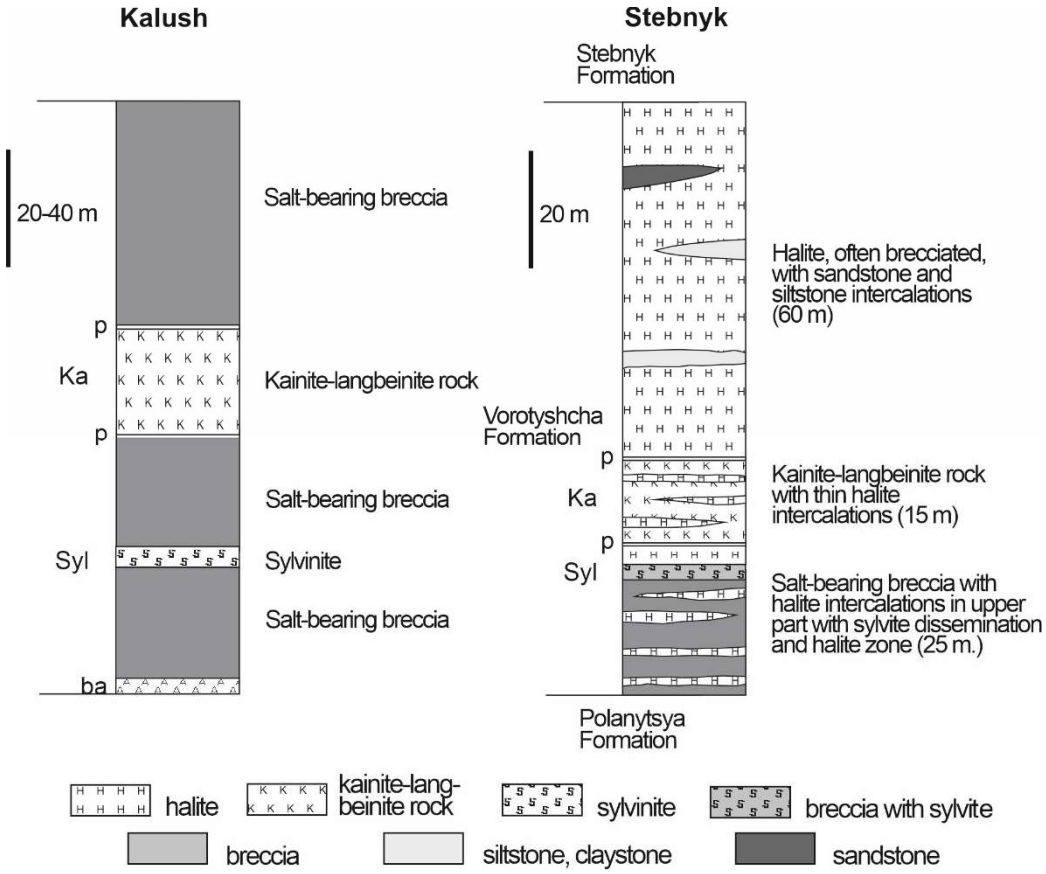

Figure 3. Presumed undisturbed lithological-stratigraphical sections of evaporites of the Holyn' fields group of the Kalysh-Holyn' deposit (after [31,37]); ba – basal anhydrite; Syl – sylvinite bed; Ka – kainite-langbeinite bed; p – polyhalite-anhydrite bed; and the Vorotyshcha Suite in the Stebnyk Mine (after [31,38]).

The potash-bearing sequence of the Kalush-Holyn deposit consists of interbedded salt claystones, salt-bearing breccias, potash and rock salt, up to 500 m thick [32] but it seems that only two beds of potash salts formed during sedimentation: the lower chloride and the upper sulphate [29–31] (Figure 3). Potash beds of the Kalush-Holyn deposit in general are composed of kainite, kainite-langbeinite (polymineralic) and langbeinite rocks; more rare is sylvinite. Clay material is dispersed and in the form of halopelite layers (clays containing up to 30% of various salts) which are interbedded with beds of potash deposits or halite. Potash beds occur in salt breccia (or salt-bearing clay) composed of fragments of clays cemented by halite. Such clay-halite rocks with silt- and clay-rich siliciclastic rocks are commonly termed "zuber" [38–40].

Evaporites of the Kalush-Holyn deposit occur close to the surface in the Dombrowo field where potash deposits are dissolved by an aquifer within Upper Pleistocene alluvial deposits, the main source of which is from rainfall [41]. A gypsum-clay caprock up to 21 m thick continues to form as indicated by Late Pleistocene-Holocene radiometric ages of hypergene salt minerals [42].

The youngest evaporite deposits in the Carpathian Foredeep Basin are of late Badenian age (see [43]). These are included, in Ukraine, in the Tyras Suite and consist of gypsum in the peripheral parts (e.g. [44–48]) laterally passing through anhydrite [49] into halite interbedded with siliciclastic deposits (e.g. [50,51]). In Poland, the latter are included in the Wieliczka Formation [52], with references therein, and in Romania in the Cosmina Formation [53], with references therein.

2. Materials and Methods

2.1. Material

 doi:10.20944/preprints202502.1716.v1

For this research we applied our previously published mineralogical data on clay minerals [17,54–61], considered here in more detail and from a different perspective. Eleven samples of the pelitic fraction of water-insoluble residue contained in the Tyras gypsum in five gypsum quarries have been studied: four quarries are in Ukraine (Shchyrets, Pisky, Verenchanka, and Nagoryany) and one in Moldova, at the boundary with Ukraine (Criva) (Figure 1). These samples represent various parts of the gypsum stratigraphic section and various lithological varieties of gypsum (stromatolitic, bedded, laminated, sabre, massive gypsum and gypsum breccia).

Twenty-three samples of the pelitic fraction of water-insoluble residue contained in the Tyras rock salt were from the Silets-Stupnytsya (boreholes 348, 671, 6 samples) and Hrynivka (borehole 525, 17 samples) localities . Ten samples of the pelitic fraction of water-insoluble residue of rock salt from the Vorotyshcha Suite (Eggenburgian) have been studied; they include samples from the following boreholes: Verkhniy Strutyn (borehole 29, 3 samples), Boryslav (borehole 17Dr, 4 samples), and Dolyna (borehole 9MD, 3 samples). The sample set from the Kalush-Holyn deposit (Holyn, Dombrovo, Northern Kainite and Khotyn fields) included 12 samples from the potash rocks (kainite, langbeinite, kainite-langbeinite, polyhalite, sylvinite), 12 from halite and halopelite layers, and 4 from salt-bearing breccia. From the Dombrovo quarry, ten samples of clays were taken from the gypsum-clay caprock: 4 of them from the northern escarpment of the quarry at the level of +265 m and 6 of them from the eastern escarpment of the quarry at the level of +277 m in boreholes 714 and 747. The thicknesses of the gypsum-clay caprock were there 4.0 and 7.5 m, respectively (Figure 4). Six samples of clays from the gypsum-clay caprock were taken from the upper, middle and lower parts of the gypsum-clay caprock above potash rocks (samples 2308, 2309, 2310) and above the salt-bearing breccia (samples 2305, 2306, 2307).

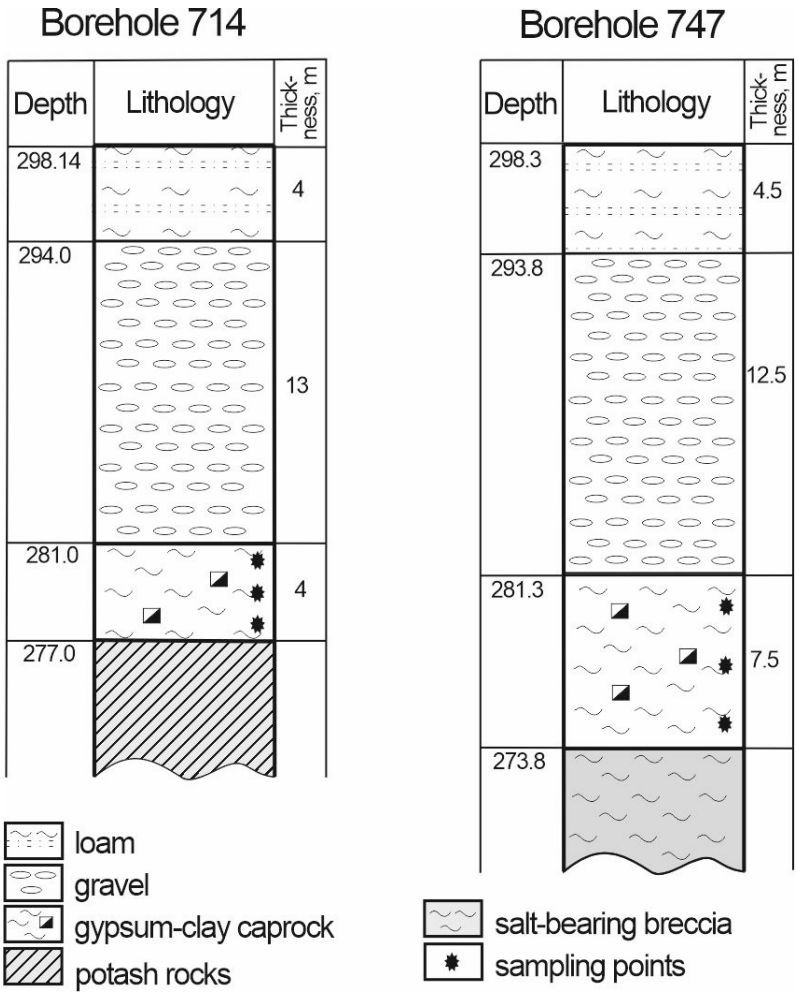

Figure 4. Sections above the potash rocks and salt-bearing breccia, Dombrovo Quarry, Kalush-Holyn deposit.

 doi:10.20944/preprints202502.1716.v1

2.2. Methods

Associations of clay minerals have been studied in the pelitic fraction by X-ray diffraction (XRD), differential thermal analysis (DTA), derivative thermogravimetry (DTG), *thermogravimetric analysis* (TG) and scanning electron microscopy (SEM).

The pelitic fraction was separated by decantation. First, evaporite samples were dissolved in distilled water and washed to complete elimination of salt minerals. From the resultant insoluble residue the sand fraction was separated and a finer fraction was washed in several steps until a stable suspension was obtained. According to the present methodology, particles smaller than 0.005 mm occur in stable suspension 40 minutes after shaking in a 5-cm-column [62]).

XRD patterns were obtained using two different powder diffractometers: DRON-0.5 and ADP-2.0. The operating conditions for DRON-0.5 were: 34 kV, 4 mA, Ni-filtered Cu-radiation, and a speed of counter movement of 2 °/min. For ADP-2.0, the operating conditions were 30-36 kV, 9-15 mA, with different wavelengths of radiation used. These included Fe-filtered Co-radiation at 0.025 2Θ/step with a counting time of 1.5 s and Mn-filtered Fe-radiation with a counting time of 0.75 s. For some samples in the 6-14 ° 2θ interval, counting times were 1.5 or 3.0 s.

Identification of clay minerals by XRD was based on the methodology of recognition of aluminosilicates in mineral associations [62,63]. To define clay minerals, oriented preparations were obtained by applying several drops of suspension of pelitic particles on a glass plate and drying at room temperature.

Oriented preparations: air-dried, ethylene-glycolated and heated at T=550 °C for 1 hour were studied. For determination of the kaolinite content in the presence of chlorite, samples were processed by a 15% solution of hydrochloric acid during a heating time of 2.5 h (T=80 °C). Chlorite minerals under such circumstances decompose completely, and kaolinite remains stable even when subjected to concentrated hydrochloric acid. Randomly oriented aggregates of pelitic particles were studied to determine the structural type of the clay minerals (060 peak position, interval 74–98 °2Θ).

Differential thermal and thermogravimetric analysis was performed on a Q-1500 D derivatograph of the Paulik-Paulik-Erdey system. The analysis was carried out at the temperature range of 20–1000 °C with a heating rate of 10 °C/min in air. Aluminum oxide served as a reference substance. Endothermic and exothermic effects recorded during such thermal analysis indicate structural features of the clay minerals, and thermal destruction by oxidation of organic matter [64].

Scanning electron microscopy (SEM) analysis was carried out with a Jeol-JSM 6490 instrument.

3. Results

3.1. Gypsum Facies

The pelitic fraction of the water-insoluble residue of the Badenian gypsum samples studied contains two main clay minerals: a considerable amount of smectite and a little illite [57]. In addition, in some samples mixed-layer chlorite-smectite and a small content of illite-smectite as well as chlorite were found (Table 1, Figure 5).

Table 1. Mineral composition of the pelitic fraction of water-insoluble residue of the Badenian gypsum in the Ukrainian and Moldavian Carpathian Foredeep basin.

Locality	Sample number	Gypsum type	Clay minerals					Other minerals
			Smectite	Chlorite-smectite	Illite-smectite	Chlorite	Illite	
Shchyrets	2313	Stromatolitic gypsum	++	–	+	–	+	Ca +
	2316	Bedded gypsum	++	(+)	–	(+)	++	Q +
	2317	Gypsum breccia	++	–	+	–	+	Ca ++

 doi:10.20944/preprints202502.1716.v1

Pisky	2319	Sabre gypsum	++	+	+	–	+	Q (+)
	2320	Grass-like gypsum	++	–	(+)	+	+	Q +,
	2321	Laminated gypsum with salin spar	+	++	+	–	+	Q (+), Fs (+)
Verenchanka (borehole 20)	822	Grass-like gypsum	++	+	(+)	–	+	Fs (+), Ca +
	20	Sabre gypsum	++	+	+	–	+	Fs (+), Do ++, Ca +
Nagoryany	818	Sabre gypsum	++	–	–	+	+	Q (+), Fs (+)
Criva (borehole 84)	102	Massive gypsum	++	(+)	+	–	+?	–
	113	Massive gypsum	+	+	+	–	–	Ca ++

Other minerals: Q – quartz; Fs – feldspar; Do – dolomite; Ca – calcite. Content in a sample: ++ considerable; + small; (+) admixture; +? presence in doubt; – mineral lacking.

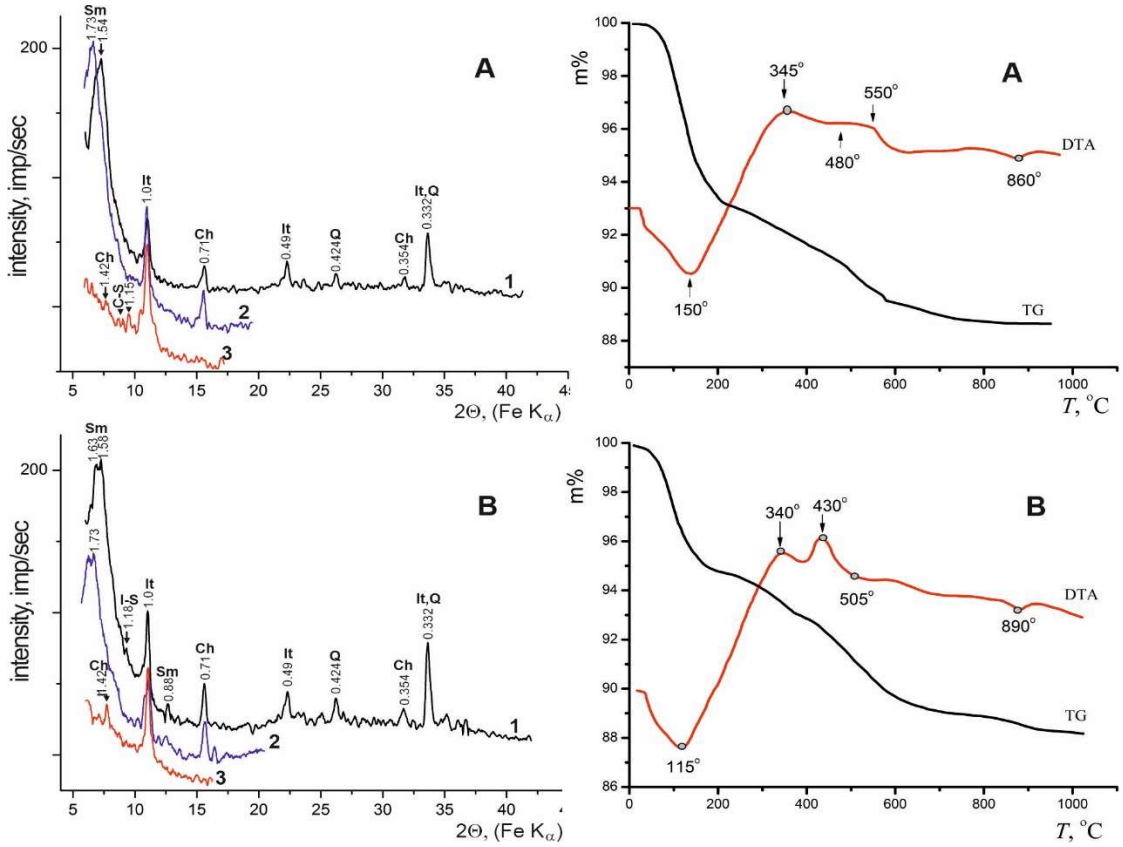

Figure 5. XRD data (left side) and DTA and TG data (right side) of the pelitic fraction of the water-insoluble residue of Badenian gypsum deposits; A – Shchyrets Quarry, sample 2316; B – Pisky Quarry, samples 2320. Left side: The smectite (001) reflection of 1.54–1.58 nm is shifted to 1.73 nm in preparations saturated with ethylene glycol. Mixed-layer illite-smectite is defined by small peak of 1.18 nm, which after saturation moved to the low-angle side. After heating, the labile packets shrank: for illite-smectite to 1.0 nm, and peaks of 1.26, 1.15 nm (within 8.8–9.6 °2Θ) indicate a chlorite-smectite admixture. Oriented preparations: 1 – air-dried, 2 – ethylene-glycolated; 3 – heated at T = 550 °C. Sm – smectite; Ch – chlorite; It – illite; mixed-layer: I-S – illite-smectite, C-S – chlorite-smectite; Q – quartz. Right side: Endothermic peak of the loss of interlayer water a by smectite and illite admixture (115, 150 °C DTA pattern), with corresponding mass loss of about 6% (TG pattern). Exothermic peaks with maxima of 340, 345 and 430 °C (DTA pattern) characterize the combustion of organic matter with corresponding mass loss of 1.3–1.9% (TG pattern). Curves: DTA – differential thermal, TG – thermogravimetric analysis.

 doi:10.20944/preprints202502.1716.v1

Smectite was recorded in all samples studied and is defined by a broad basal reflection (001) of high intensity. In some samples this diffractional maximum is split at the apex, with interlayer spaces at 1.51–1.58 and 1.63 nm, that when ethylene-glycolated are shifted to 1.68–1.71 and 1.73 nm, respectively. The broadening of the (001) reflection with a release of the 1.63 nm line on the diffraction picture of the air-dried preparation is an indication of two minerals of the smectite group (Figure 5). The position of the (060) reflection of preparations of randomly oriented pelitic particles at 0.149–0.150 nm indicates a dioctahedral type of smectite structure although in that interval a weakly-expressed 0.153 nm reflection also occurs that can indicate an admixture of trioctahedral smectite. A trioctahedral structure similarly may indicate chlorite but this reflection was recorded also in samples were chlorite is absent. Thus, smectite in the pelitic fraction is heterogeneous: there occurs a mixture of Al-Fe dioctahedral allogenic, and a small quantity of Mg trioctahedral authigenic, material [57]. In thermally treated preparations reflections at 1.51–1.63 nm are shifted to 0.98 nm, and in some preparations, in the area of low angles, there are additional reflections of small intensity and poor separability which correspond to chlorite and chlorite-smectite (Figure 5). Illite was recorded in most samples but its content is small. It was diagnosed based on 0.98, 0.49, and 0.332 nm reflections that do not change their location in ethylene-glycolated conditions and during thermal treatment. Illite corresponds to a dioctahedral structure type but the interlayer space of the (060) reflection at 0.149 nm is superimposed on the same reflection of smectite.

On the DTA curve a profound low-temperature endothermic effect of the loss of interlayer water is noted in the temperature range of 115–150 °C. It corresponds to a mass loss (5.1–6.9%, Figure 5 according to the TG curve) by smectite, which dominates in the samples, and by illite as well as mixed-layer chlorite-smectite and illite-smectite, which are present in small amounts. Illite on the DTA curves shows a low-temperature endo-effect that corresponds to the loss of interlayer water and is superimposed on the endo-effect of smectite across the whole temperature range. Since interlayer intervals of illite are able to include a smaller amount of water molecules and to release them at somewhat lower temperature (compared to smectite), on the DTA curve a weak endo-effect in the range of 500–700 °C corresponds to the release of constitutionally bound water from the smectite structure (1.5–2.7%) as well as from illite and mixed-layer phases. The small endo-effect, in the temperature range of 800–900 °C, corresponds to release of the residue of constitutionally bound water and destruction of the structure. In the case of subsequent temperature increase from the decomposition products, a new mineral crystallises and this is expressed by the appearance of an exo-effect on the DTA curve (Figure 5) [65]. Exothermic peaks in the region of 300–480 °C (DTA curve) characterize the combustion of organic matter with corresponding mass loss of 1.3–1.9% (TG curve).

An SEM microphotograph (Figure 6A) shows the crystal shape of smectite from the pelitic fraction of water insoluble residue of the Badenian gypsum.

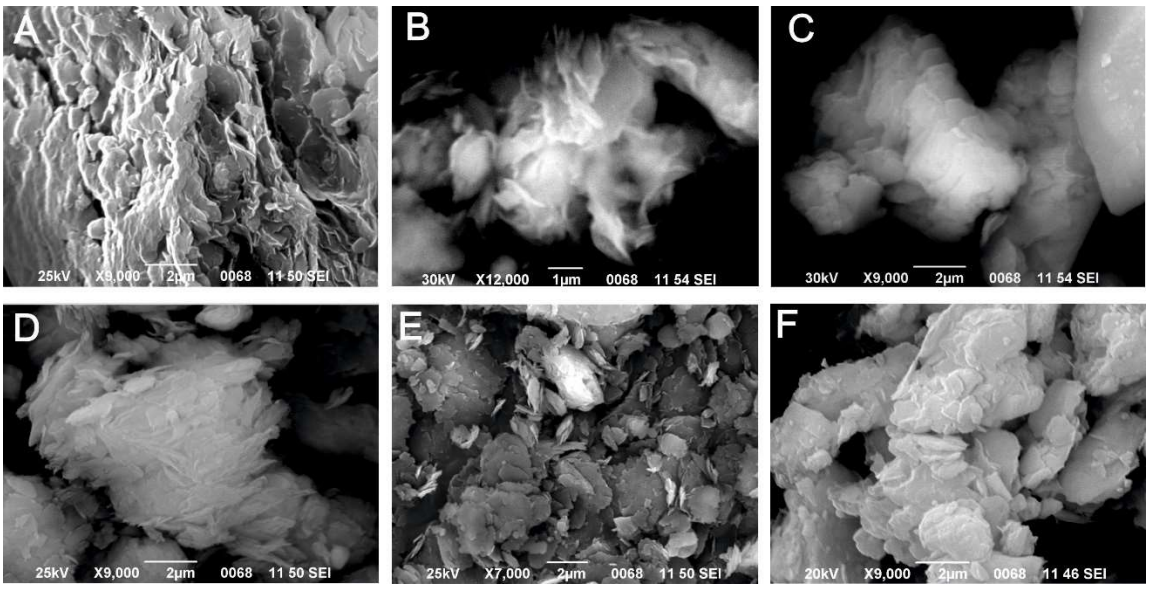

 doi:10.20944/preprints202502.1716.v1

Figure 6. SEM microphotographs of clay minerals of the pelitic fraction of water-insoluble residue of Badenian gypsum (A– Pisky Quarry, sample 2320) and Badenian rock salt (B and C – Hrynivka 525 borehole, sample 1357) as well as SEM microphotographs of illite in the pelitic fraction of water-insoluble residue of Eggenburgian rock salt (D, E – Boryslav 17 Dr borehole, sample 2570) and Badenian rock salt (F – Hrynivka 525 borehole, sample 1350). A – smectite – leaf-like curved plates with bright rims; B – smectite – semi-transparent twisted and bent plates; C – corrensite – aggregates of ordered pseudohexagonal plates; D – illite – elongated plates with sharp, locally split, ends within an aggregate; E – illite – isometric plates with uneven contours; F – illite – aggregates of isometric plates.

3.2. Halite Facies

Illite, chlorite and mixed-layer illite-smectite occur in rock salt of Eggenburgian age (Vorotyshcha Suite). In addition to those minerals, trioctahedral smectite and mixed-layer chlorite-smectite occur in Badenian rock salt (Tyras Suite), and, at the Hrynivka and Silets-Stupnytsya sites, corrensite was also recorded (Table 2, Figure 7).

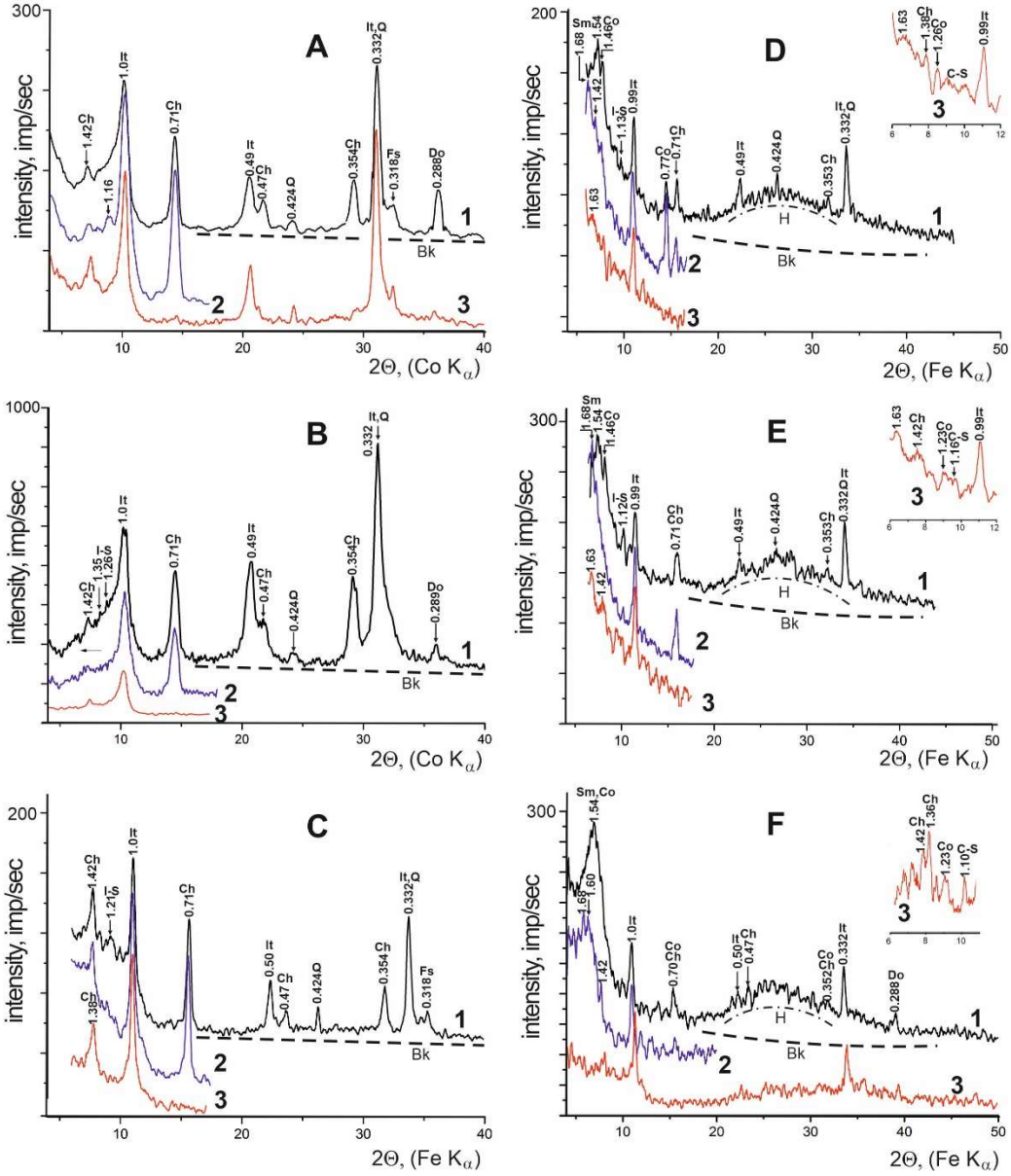

Figure 7. XRD data of the pelitic fraction in water-insoluble residue of Eggenburgian (A-C) and Badenian rock salt (D-F). After heating (curves 3), reflections at 1.23 and 1.26 nm suggest the presence of corrensite, and in the range of 1.23–0.99 nm – chlorite-smectite with predominantly smectite packets; D,E,F – the convex raised

 doi:10.20944/preprints202502.1716.v1

background (halo) is a sign of adsorption of amorphous organic compounds on clay particle surfaces. A – Verkhniy Strutyn 29 borehole, sample 2574; B – Boryslav 17Dr borehole, sample 2570; C – Dolyna 9MD borehole, sample 863; D – Silets-Stupnytsya 671 borehole, sample 48; E – Silets-Stupnytsya 348 borehole, sample 902; F – Hrynivka 525 borehole, sample 1357. Oriented preparations: 1 – air-dried; 2 – ethylene-glycolated; 3 – heated at T = 550 °C; Sm – smectite; Co – corrensite; Ch – chlorite; It – illite; mixed-layer: I-S – illite-smectite, C-S – chlorite-smectite; Q – quartz; Do – dolomite; Fs – feldspar; Bk – machine background, H – halo.

Table 2. Mineral composition of the pelitic fraction of water-insoluble residue, rock salt of the Ukrainian Carpathian Foredeep.

Sample number	Depth [m]	Clay minerals						Other minerals
		Smect-ite	Corren-site	Chlorite-smectite	Illite-smectite	Chlor-ite	Illite	
Borehole 29, Verkhniy Strutyn, Vorotyshcha Suite								
2573	562	–	–	–	+	++	++	Q (+), Fs –, Do –, Ca –, Ma –
2574	626	–	–	–	+	++	++	Q (+), Fs (+), Do +, Ca –, Ma –
2575	698	–	–	–	++	++	++	Q (+), Fs +, Do –, Ca –, Ma –
Borehole 17Dr, Boryslav, Vorotyshcha Suite								
2567	352	–	–	–	–	++	++	Q +, Fs +, Do –, Ca –, Ma ++
2566	353	–	–	–	–	++	++	Q ++, Fs +, Do –, Ca –, Ma +
2569	377	–	–	(+)	+	++	++	Q +, Fs (+), Do (+), Ca –, Ma –
2570	409	–	–	–	+	++	++	Q (+), Fs –, Do (+), Ca –, Ma –
Borehole 9MD, Dolyna, Vorotyshcha Suite								
858	38	–	–	+?	+	++	++	Q –, Fs (+), Do (+), Ca –, Ma –
859	73	–	–	–	+	++	++	Q +, Fs (+), Do –, Ca –, Ma –
863	152	–	–	–	+	++	++	Q (+), Fs (+), Do –, Ca –, Ma –
Boreholes 348 and 671, Silets-Stupnytsya, Tyras Suite								
902	132	+	+	+	+	+	+	Q (+), Fs–, Do –, Ca –, Ma –
907	172.5	–	–	++	+	+	+	Q +,Fs –, Do +, Ca –, Ma –
58	272	+	–	++	+	(+)	+	Q +, Fs –, Do +, Ca –, Ma –
54	302	–	–	++	(+)	+	+	Q (+), Pt –, Do +, Ca –, Ma –
47	449	+?	–	++	+	(+)	+	Q (+), Pt –, Do +, Ca –, Ma –
48	464	+	+	+	(+)	(+)	+	Q +, Fs Do –, Ca –, Ma –
Borehole 525, Hrynivka, Tyras Suite								
1342	304	+	++	+	(+)	+	+	Q +, Fs (+), Do –, Ca –, Ma –
1344	310.1	+	+	+	+	+	+	Q +, Fs (+), Do –, Ca –, Ma –
1348	330	+?	–	++	(+)	(+)	+	Q +, Fs –, Do –, Ca –, Ma –
1350	342	+	+?	++	+	(+)	+	Q (+), Fs (+), Do +, Ca +, Ma –
1352	362	+	+?	++	(+)	(+)	+	Q (+), Fs –, Do ++, Ca –, Ma –
1354	376	–	–	++	+	+	++	Q +, Fs (+), Do +, Ca +, Ma –
1356	395–399	+	++	(+)	–	(+)	++	Q +, Fs –, Do +, Ca –, Ma –
1357	410–411	+	++	+		+	+	Q–, Fs–, Do +, Ca –, Ma –
1361	444–448	+	++	(+)	(+)	(+)	+	Q (+), Fs (+), Do +, Ca –, Ma –

 doi:10.20944/preprints202502.1716.v1

1362	454–456	++	+?	(+)	+	+	+	Q (+), Fs –, Do +, Ca –, Ma –
1364	474	+	++	+	–	(+)	+	Q (+), Fs –, Do +, Ca –, Ma –
1365	480	+?	++	+	+	(+)	+	Q –, Fs –, Do +, Ca –, Ma –
1366	489	–	+?	++	–	+	++	Q (+), Fs –, Do +, Ca –, Ma –
1369	518	++	++	(+)	–	(+)	+	Q (+), Fs (+), Do +, Ca –, Ma –
1370	521–528	+	–	++	+	(+)	++	Q +, Fs (+), Do +, Ca +, Ma –
1371	532	+	+?	++	(+)	+	+	Q +, Fs (+), Do –, Ca –, Ma –
1372	536	+	–	++	+	+	++	Q +, Fs (+), Do –, Ca –, Ma –

Other minerals: Q – quartz, Fs – feldspar, Do – dolomite, Ca – calcite, Ma –magnesite; Content in a sample: ++ considerable; + small; (+) admixture; +? presence in doubt; – mineral lacking.

Clay minerals of both suites studied contain dioctahedral illite and trioctahedral chlorite that are indicated by reflections (060) at 0.149 and 0.153 nm; for both of them Fe-Mg-chlorite is recorded. Its composition is indicated by smaller intensities of the first and third basal reflections by comparison with the second one. Illite and chlorite from the Eggenburgian rock salt has intense, distinct basal reflections (Figure 7A-C) indicating that these are well crystallised, while in the Badenian rock salt illite is characterized by a considerable asymmetry of the first basal reflection at 1.0 nm in the area of small angles that could have resulted from poor crystallisation, a content of interlayer water or swelling packets (Figure 7D-F). Clay minerals of the Badenian rock salt contain more swelling minerals than the Eggenburgian rock does. Mixed-layer illite-smectite was diagnosed by small reflections in the field of 1.12–1.28 nm that in ethylene-glycolated preparations was shifted to 1.46 nm. Chlorite-smectite was diagnosed by a series of 1.42–1.51 nm reflections shifted to 1.60–1.71 nm.

Smectite is diagnosed by the behaviour of (001) reflections with an interlayer distance of 1.51–1.55 nm in air-dried preparations that in ethylene-glycolated are shifted to 1.71 nm and in diffractograms of thermally-treated samples decreased to 0.98 nm. This diffraction maximum has various forms and a series of low-intensity lines of poor resolution that indicate a content of chlorite packets in the smectite structure [65]. Corrensite is established by reflections: 1.42–1.46; 0.70-0.77; 0.472; 0.353 nm on diffractograms of air-dried preparations, in ethylene-glycolated ones they acquire values of 1.60; 0.78; 0.355 nm, and on the diffractograms of preparations heated at 550 °C reflection in the field 1.23–1.26 nm is observed. A reflection of 2.88 nm is reported for corrensite in the literature; on the diffractograms of the samples studied it has the form of an inflection or is completely absent, which may indicate some disorder in the corrensite structure [65].

On the X-ray curves of the pelitic fraction of the Eggenburgian and Badenian rock salt, the area of low angles is fixed by a series of reflections that do not cover the diffraction from the basal planes of the clay structures. These reflections do not change their position in ethylene-glycolated conditions, and part of them remains on diffractograms after thermal processing (Figure 8) [60].

 doi:10.20944/preprints202502.1716.v1

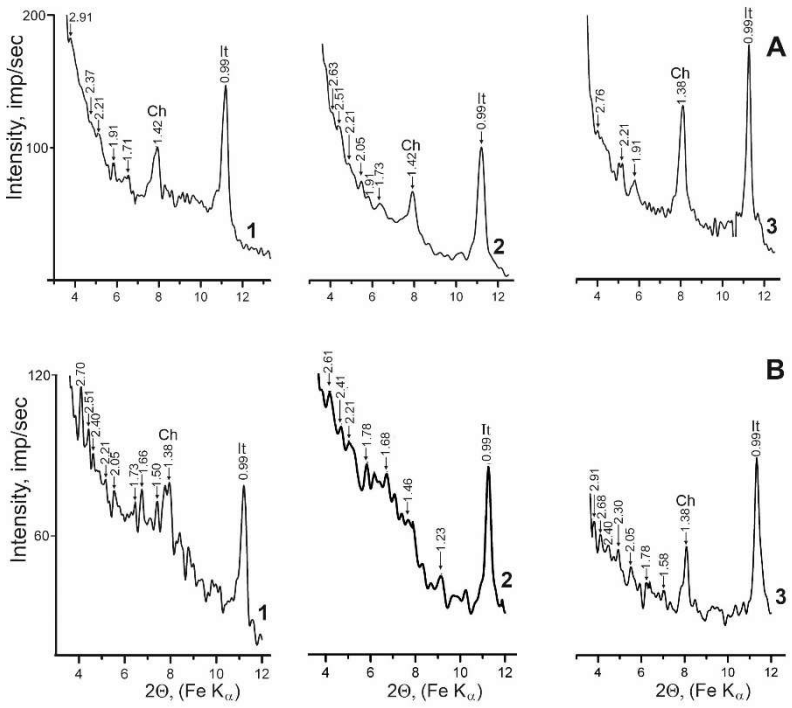

Figure 8. XRD data in the area of small angles of the pelitic fraction in water-insoluble residue of the Eggenburgian (A – Dolyna 9MD borehole, sample 863) and Badenian (B – Hrynivka 525 borehole, sample 1354) rock salt. Scattered lines of low intensity with d 1.73–2.91 nm indicate the existence of interlayer spaces of clay structures filled with organic compounds (curves 1, 2). Organic matter trapped in the structure, resistant to high temperature processing (lines with d 2.91–1.58 nm of the region 3–7 °2Θ in the diffractogram, curves 3). Oriented preparations: 1 – air-dried; 2 –ethylene-glycolated; 3 – heated at T = 550 °C. It – illite, Ch – chlorite.

All diffraction spectra of the pelitic fraction of the Badenian rock salt show an increased position of line of background and a halo with a large number lines of low intensity and poor separability in the area of the 22–36 degree 2Θ, Fe Kα radiation (Figure 7D-F). In addition, the first two basal reflections (001) and (002) are extended at the base, and their intensity is too low for the main lines of minerals which prevail in a sample. In the area of low angles of diffraction, distinct peaks of low intensity with interlayer distances 2.91–1.54 nm are recorded that, however, do not coincide with the reflection (001) of corrensite – 2.84 nm. Thus, on diffractograms of air-dried and ethylene-glycolated preparations distinct lines 2.70; 2.61; 2.51; 2.40–2.37; 2.21; 2.05; and 1.91 nm are recorded, and among these the reflections 2.73–2.70; 2.51; 2.21 and 2.05 nm are particularly frequent; at the Hrynivka site they occur on all diffraction curves (air-dried or ethylene-glycolated). After the thermal treatment (T = 550 °C) distinct peaks remain: 2.76–2.63; 2.40–2.30; 2.05; 1.78-1.58 nm (Figure 8).

Diffractometric curves of oriented preparations of the pelitic fraction from the Eggenburgian rock salt showed that these sites lack a marked halo and increased background (which is characteristic of the Badenian rock salt) (Figure 7A-C). On the DTA curve of the pelitic fraction of water-insoluble residue of the Eggenburgian and Badenian rock salt, a distinct low-temperature endo-effect is noted with a maximum (110–140 °C) which corresponds to the loss of interlayer water (1.8–3.4 % as the mass loss on the TG curve). On Figure 9 for the Eggenburgian rock salt, sample 2570, which contains illite, chlorite and a small amount of illite-smectite the loss of interlayer water is 3.4 % (Figure 9A), while for Badenian rock salt, sample 902, in which small amounts of illite, chlorite as well as swelling minerals and phases – smectite, corrensite, chlorite-smectite and illite-smectite – are present, the loss of interlayer water is smaller at 2.4 % (Figure 9B). The small loss of interlayer water was caused by the presence of captured organic compounds in interlayer spaces of those labile structures. The exothermic effect in the temperature interval of 230–480 °C corresponds to a process of thermooxidative destruction of organic matter related to clay particle surfaces. Endothermic effects

 doi:10.20944/preprints202502.1716.v1

at the DTA curves within 480–810 °C correspond to dehydroxilation, i.e. discharge of constitutional water of clay minerals and structural destruction. Also, organic compounds sorbed by interlayer spaces are lost in this temperature interval (Figure 9).

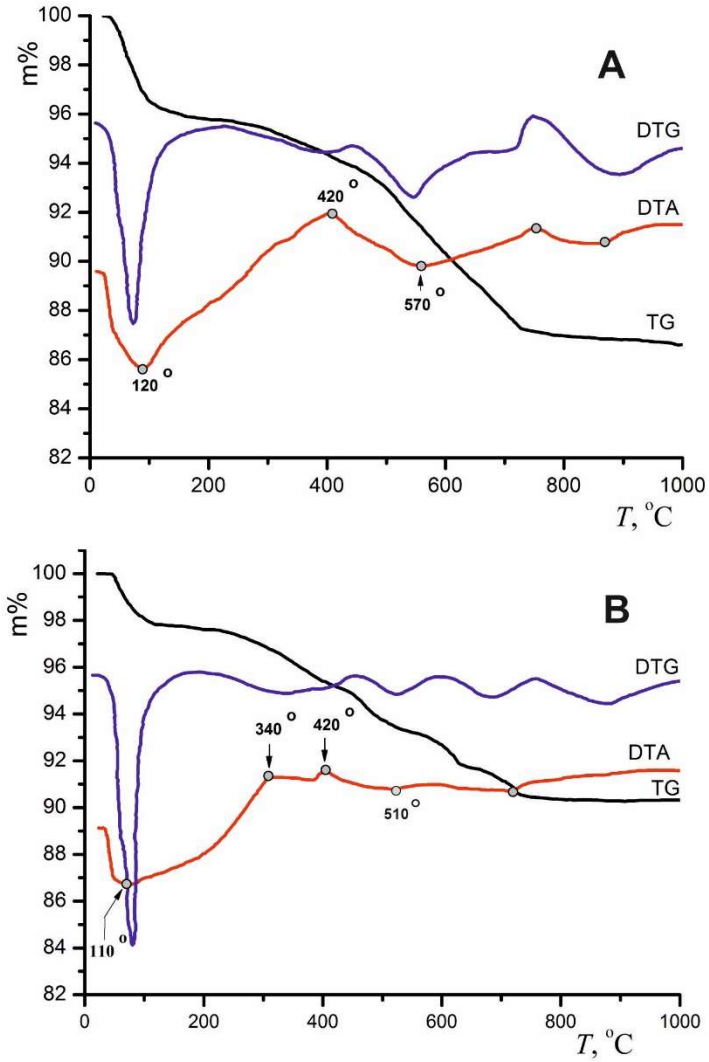

Figure 9. DTA-TG data for the pelitic fraction of water-insoluble residue of the Eggenburgian (A – Boryslav 17Dr borehole, sample 2570) and Badenian (B – Silets-Stupnytsya 348 borehole, sample 902) rock salt. A – endothermic peak is due to the loss of interlayer water by an illite and illite-smectite admixture at 120 °C (DTA pattern), with corresponding mass loss of about 3.4% (TG pattern); B – endothermic peak of the loss of interlayer water by clay minerals at 110 °C (DTA pattern), with corresponding mass loss of about 2.4% (TG pattern); the insignificant mass loss is due to replacement of part of the interlayer water by organic compounds in the interlayer spaces of labile minerals. Curves: DTA – differential thermal, DTG – differential thermogravimetric, TG – thermogravimetric analysis.

According to our SEM data the pelitic fraction of the halite facies mostly consists of particles 2–4 μm in size, although some tabular and bulky particles as small as 0.5 μm are present. SEM microphotographs show smectite, corrensite (Figure 6B,C) and illite (Figure 6D-F).

3.3. Potash Facies

The association of clay minerals of the Miocene potash facies of the Carpathian Foredeep is composed of illite and chlorite (Table 3, Figure 10). Chlorite in the Kalush-Holyn deposit is a trioctahedral Fe-Mg (more rarely a Mg-Fe) mineral. Dioctahedral illite in these deposits is characterized by structural ordering that is expressed by the form of the first basal reflection and its

 doi:10.20944/preprints202502.1716.v1

location on the diffractogram. The 001 reflections of illite from the salt-bearing breccia are widened on their low-angle side, while those from the potash rocks are sharp and symmetrical; for some of them (kainite-langbeinite rocks) that reflection is relatively narrow (of small width), and enabled diagnosis of that mineral as mica [54,59]. It is not fully explained to what extent those were structurally ordered. In the potash rocks, illite is transformed into mica either fully [66] or partially [54]. By mica we mean a stable, ordered form of illite with a small K^+ deficit in the interlayer intervals. For such mica-like clay minerals the following terms are commonly applied: illite $2M_1$ or muscovite $2M_1$. We use the term "mica" because the determination of polytype structures was not applied. Our study of diffractograms of pelitic fraction of the potash-bearing rocks of both air-dried and ethylene-glycolated preparations show that the basal 001 reflections are bifurcated at the top, with (d) 0.99 and 1.0 nm (Figure 10A4,B4). Our results suggest that illite as well as mica is present in the pelitic fraction. When scanning in slow motion at angles of 8–13 °2Θ in diffractograms, clear splits are seen (see Figure 10A4,B4) which indicates the occurrence of the structurally similar minerals, mica and illite.

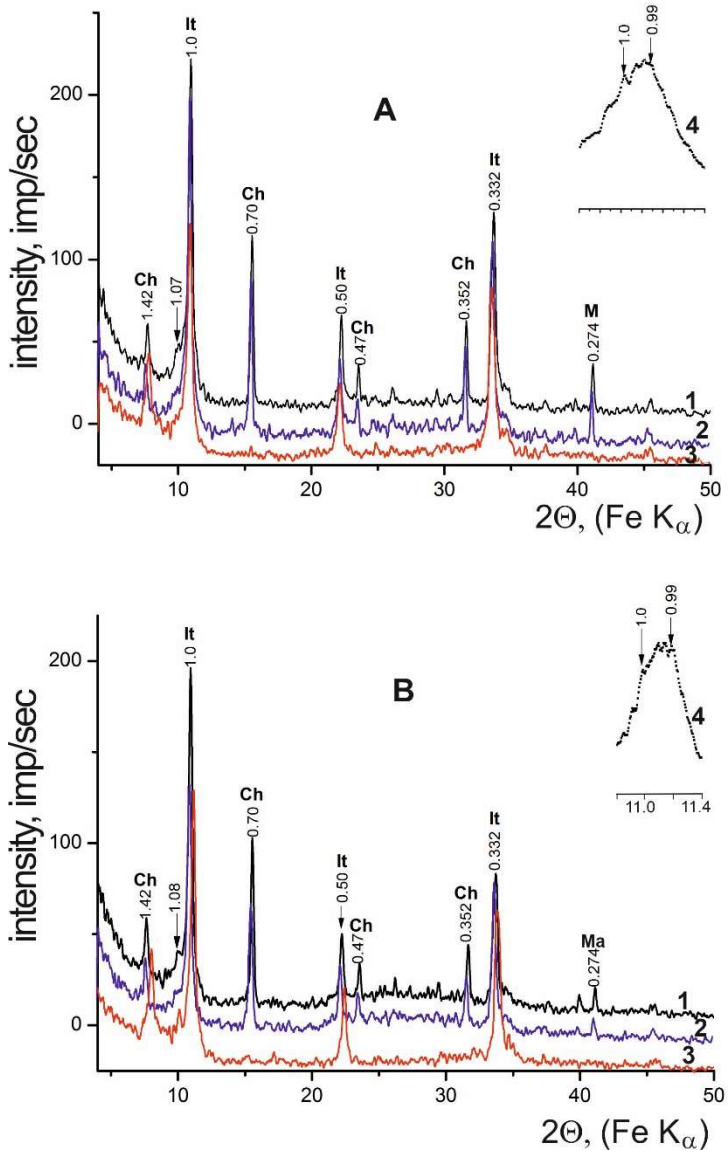

Figure 10. XRD data of the pelitic fraction of water-insoluble residue from the potash facies of the Kalush-Holyn potash deposit. Intense, narrow basal reflections of illite and chlorite indicate that these are well crystallised. The reflections at 1.07 nm (at angles of 10.4 °2Θ) is the basal reflection of mica, in the interlayer space of which relic hydrated K^+ cations are still present. A split 001 reflection (scanning in slow motion – 4), indicates the occurrence of the structurally similar minerals, mica and illite. A – halite from alternation of halite and halopelite layers,

 doi:10.20944/preprints202502.1716.v1

Holyn, sample 2185; B – langbeinite rock, Dombrovo, sample 2250. Oriented preparations: 1 – air-dried; 2 – ethylene-glycolated; 3 – heated at T = 550 °C; 4 – part of the diffraction curve scanned in slow motion. It – illite; Ch – chlorite; Ma – magnesite.

Table 3. Mineral composition of the pelitic fraction of water-insoluble residue of potash rocks and salt- bearing breccia from the potash facies of the Kalush-Holyn potash salt deposit.

Locality	Sample number	Lithology	Clay minerals		Other minerals
			Illite	Chlorite	
Dombrovo	3	Clayey kainite rock	++	++	–
Northern Kainite field	1006в	Kainite rock	++	++	–
Northern Kainite field	1029	Kainite rock	++	++	–
Dombrovo	2251	Kainite rock	++	++	Ma+
Dombrovo	2	Langbeinite rock	++	++	*
Dombrovo	1105	Langbeinite rock	++	++	*
Dombrovo	2250	Langbeinite rock	++	++	Ma+
Dombrovo	1	Kainite-langbeinite rock	++	++	Ma+
Dombrovo	1097a	Kainite-langbeinite rock	++	++	Ma+
Dombrovo	2249	Kainite-langbeinite rock	++	++	Ma+
Khotyn field	1017	Sylvinite	++	++	Ma+
Dombrovo	5	Clayey polyhalite rock	++	++	–
Northern Kainite field	1006a	Salt-bearing breccia	++	++	Ma+
Khotyn field	1019	Salt-bearing breccia	++	++	–
Dombrovo	1117	Salt-bearing breccia	++	++	–
Holyn	2219	Halite from salt-bearing breccia	++	++	Ma+
Holyn	1035	Greenish-grey halite from the potash rocks	++	+	–
Holyn	1039	Greenish-grey halite from the potash rocks	++	+	Ma+
Dombrovo	1097	Greenish-grey halite from the potash rocks	++	+	Ma+
Dombrovo	14	Halite from alternated halite and halopelite layers	++	+	Ma+
Dombrovo	15	Halite from alternation of halite and halopelite layers	++	+	Ma+
Holyn	2185	Halite from alternated halite and halopelite layers	++	++	Ma+
Northern Kainite field	1026	Halite from alternated halite and halopelite layers	++	+	–
Holyn	1060	Greenish-grey halite from alternated halite and halopelite layers	++	+	–
Holyn	1062	Halite from alternated halite and halopelite layers	++	+	*

 doi:10.20944/preprints202502.1716.v1

Dombrovo	25	Halopelite from alternated halite and halopelite layers	++	+	Ma+
Dombrovo	1096	Halopelite from alternated halite and halopelite layers	++	+	*
Dombrovo	1104	Halopelite from alternated halite and halopelite layers	++	+	–

Other minerals: Ma – magnesite, * – carbonate not determined. Content in a sample: ++ considerable; + small; – mineral lacking.

Thermogravimetric analysis of the pelitic fraction of potash rock at low temperature (up to 200 °C) showed an endothermic effect due to the loss of interlayer water by illite, indicating a mass loss of almost 1% (Figure 11B). Such a small loss of interlayer water at a significant content of illite in the sample corroborates the XRD data indicating that the mica-like mineral with a reflection at 1.0 nm is composed of illite and mica. A high-temperature endothermic effect with a maximum at 575 °C in the DTA curve, which is accompanied by a 9.4% mass loss in the TG curve, is responsible for the dehydroxilation of illite and chlorite as well as magnesite dissociation (Figure 11B).

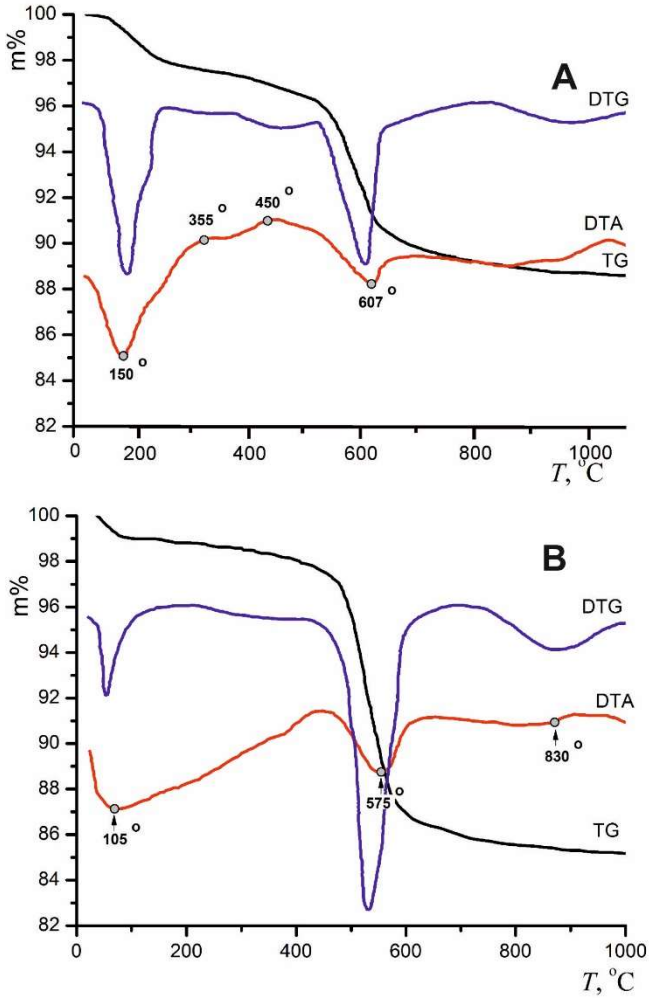

Figure 11. DTA-TG data for the pelitic fraction of water-insoluble residue from the potash facies of the Kalush-Holyn potash deposit. A – endothermic peak due to the loss of interlayer water by illite at 150 °C (DTA pattern), with corresponding mass loss of about 3.2% (TG pattern); halite from salt-bearing breccia, Holyn, sample 2219;

 doi:10.20944/preprints202502.1716.v1

B – the endothermic effect of the loss of interlayer water by illite (105 °C, DTA pattern) corresponds to a mass loss of about 1% (TG pattern) and the effect of dehydroxylation of clay minerals and of magnesite dissociation corresponds to a loss of mass of 9.4% (TG pattern); kainite rock, Dombrovo, sample 2251. Curves: DTA – differential thermal, DTG – differential thermogravimetric, TG – thermogravimetric analysis.

On the SEM microphotographs the pelitic fraction of the potash facies (Figure 12) are observed particles of both clay and pelitic dimension, and in places aggregates of particles. The pseudohexagonal particles in Figure 12D may be $2M_1$ mica, and isometric particles with smoothened outlines may be illite.

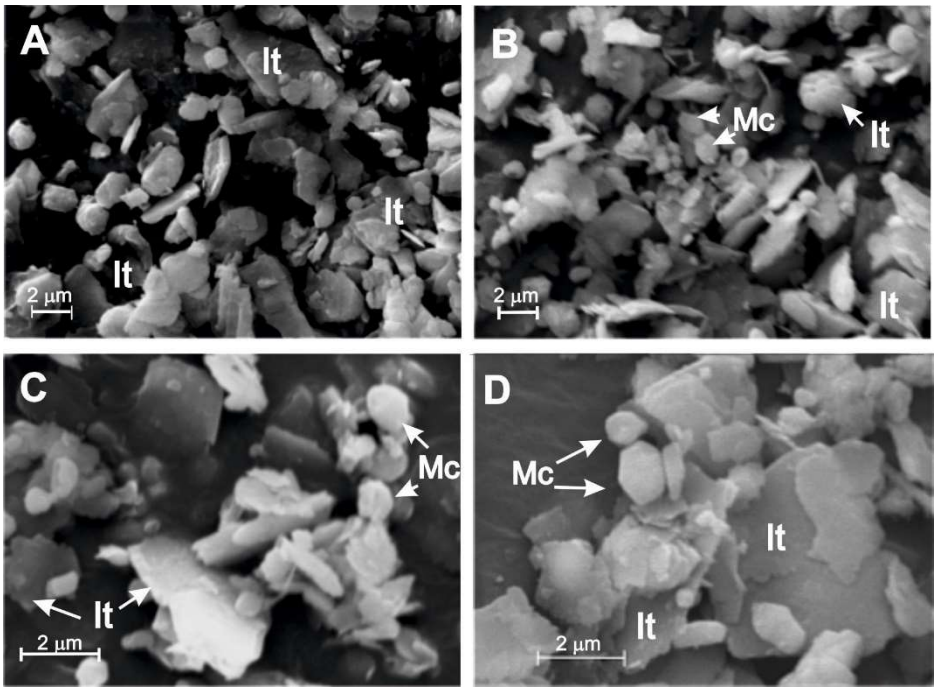

Figure 12. SEM microphotographs of clay minerals in the pelitic fraction of water-insoluble residue of the potash facies of the Kalush-Holyn potash deposit. Morphology of illite (It) and mica (Mc): illite particles are of isometric shape; the pseudo-hexagonal-shaped particles are supposedly mica. A – halite of salt-bearing breccia (Holyn, sample 2219), B – kainite-langbeinite rock (Dombrovo, sample 2249), C – kainite rock (Dombrovo, sample 2251), D – halite from alternation of halite and halopelite layers (Holyn, sample 2185).

3.4. Weathering Zone of the Kalush-Holyn Deposit

Our data indicate that the association of clay minerals in the hypergene deposits – in gypsum-clay caprock, above potash rocks and salt-bearing breccia – contain, in addition to illite and chlorite, consistently mixed-layer illite-smectite, and in five samples kaolinite was additionally found that was not recorded in the evaporite deposits before dissolution (Table 4).

Table 4. Mineral composition of the pelitic fraction of water-insoluble residue of the weathering zone of the Kalush-Holyn potash salt deposit, Dombrovo quarry.

Sample number	Lithology	Clay minerals				Other minerals
		Illite	Chlorite	Illite-smectite	Kaolinite	
Clays from the gypsum-clay caprock above potash rocks						
2253	Clay with gypsum	++	++	+	–	Ma+
2255	Clay with syngenite	++	++	+	–	–
2257	Clay with mirabilite	++	++	+	–	Ma+
2300	Clay with syngenite	++	++	+	–	Ma+

 doi:10.20944/preprints202502.1716.v1

2308	Grey clay, upper part of the gypsum-clay caprock	++	++	+	+	–
2309	Grey clay, middle part of the gypsum-clay caprock	++	++	+	+	–
2310	Grey clay, lower part of the gypsum-clay caprock	++	++	+	+	–
	Clays from the gypsum-clay caprock above the salt-bearing breccia					
2305	Grey clay, upper part of the gypsum-clay caprock	++	++	+	+	–
2306	Grey clay with gypsum and syngenite, middle part of the gypsum-clay caprock	++	++	+	–	–
2307	Grey clay, lower part of the gypsum-clay caprock	++	++	+	+	Ma+

Other minerals: Ma – magnesite. Content in a sample: ++ considerable; + small; – mineral lacking.

A mixed-layer phase shows a considerable asymmetry of the first basal reflection of 1.0 nm in the area of low angles and small reflections at 1.04–1.28 nm. In ethylene-glycolated preparations, the width of the basal line (001) of illite diminishes and the additional reflections decrease on its low-angles side to 1.51 nm and can be traced between reflections at 1.0 and 1.7 nm. All this gives an opportunity to diagnose such a mixed-layer phase as illite-smectite mainly of illite composition with a small proportion of smectite [67].

The first basal reflection of illite is shifted from its low-angles side by an admixture of mixed-layer phase. The location of line (060) (0.149–0.150 nm) indicates that illite in the gypsum-clay caprock is dioctahedral.

Reflection 1.38–1.40 nm does not change the location on diffractograms of ethylene-glycolated preparations, therefore, this line is the basal reflection (001) of chlorite. The location of line (060) on diffractograms of preparations of randomly oriented pelitic particles (0.153–0.155 nm) indicates that chlorite in the gypsum-clay caprock is trioctahedral.

A clearly defined line 0.70 nm, available on diffractograms of samples subject to solution by hot HCl, indicates the presence of kaolinite. It was recorded in half of the samples of gypsum-clay caprock studied.

4. Interpretation

4.1. Brine Concentration Control

We consider that the most important factor in the transformation of clay minerals is the brine concentration [7,8] and the higher the water mineralization, the more advanced are the transformation processes [1]. An increased brine concentration causes aggradational transformation of clay minerals: changes involving structural ordering through the capture of cations and a decrease in molecular volume. This is clearly supported by the example of transformation of unstable and labile minerals and phases (kaolinite, smectite and mixed-layer phases) that pass into illite and chlorite, these minerals being stable in an evaporite environment. Kaolinite is stable in acid conditions at pH ~5 [68]. In an evaporite basin pH conditions depend on brine concentration: the pH value at the sulphate-carbonate stage is ~8.6 and decreases to 7.0–7.5 at the halite stage [69]. In evaporite deposits, kaolinite is destroyed in the middle of the halite stage; in deposits of higher stages it occurs very rarely [70]. As well as kaolinite destruction, its illitization is possible [71], but this process has not been proven in marine conditions [5]. The clay mineral assemblage of the Badenian gypsum is represented mainly by allogenic clay minerals (dioctahedral smectite, illite, rarely chlorite) and it indicates a relatively low brine concentration in the evaporite basin. The presence of a small content of authigenic minerals (trioctahedral smectite and illite), and mixed-layer chlorite-smectite and illite-

 doi:10.20944/preprints202502.1716.v1

smectite, indicates the beginning of aggradational transformation processes [57]. Smectite in evaporite basins has two modes of provenance: allogenic, dioctahedral smectite from the land, while trioctahedral smectite forms through the decomposition of volcanic glass of pyroclastic material, where volcanism is coeval with salt accumulation. Thus, transformation of smectite occurred through mixed-layer illite-smectite and chlorite-smectite to dioctahedral illite and trioctahedral chlorite [5,65]. At the sulphate-carbonate stage of halogenesis the content of potassium ion increases from 1.5 to 3.9 g/l [72] so at this stage the transformation of unstable allogenic clay minerals was only initiated. However, the concentration of brines from which the Badenian gypsum precipitated was considerably lower due to an important inflow of continental water into the Badenian evaporite basin [73–77]. The low concentration of K^+ and Mg^{2+} ions caused a slow transformation of unstable clay minerals.

The clay mineral association in the Badenian rock salt (Hrynivka and Silets-Stupnytsya sites) contains minerals with labile (swelling) structures: smectite, corrensite and mixed-layer chlorite-smectite with an admixture of illite, chlorite and illite-smectite. Such an association of clay minerals is consistent with the influence of contemporaneous volcanism [17,56,60]. During the decomposition of volcanic glass of pyroclastic material that entered the salt basin, trioctahedral smectite was formed that was subject to further transformation through mixed-layer phases into chlorite, this being the end product of a number of transformations [65]. This interpretation explains the presence of a considerable number of swelling clay minerals, but it does not answer why they did not transform in the Badenian salt-forming basin under the influence of brines.

One of the reasons may be low brine concentrations. Geochemical conditions in the Miocene evaporite basins of the Ukrainian Carpathian Foredeep were influenced by substantial inflow of continental water [73–80]. Low concentrations of K^+ and Mg^{2+} ions caused slow transformation of unstable clay minerals. Authigenic trioctahedral Mg-smectite is the initial clay mineral at the sulphate-carbonate stage of halogenesis (e.g. [10,65] and due to its transformation through intermediate mixed-layer phases, a number of clay minerals originated.

In the Eggenburgian and Badenian rock salt, the brine concentration during halite precipitation was determined through the use of an ultramicrochemical method [75 and references therein] that indicated, at the Hrynivka site, a low brine concentration from which the halite crystallised [56]. In the Silets-Stupnytsya site, although halite crystallised from brines of high concentration, the association of clay minerals is the same as in the rock salt of the Hrynivka site. So, it is insufficient to explain the considerable content of swelling clay minerals in the Badenian rock salt only by the influence of brine concentration on the transformation of clay minerals. In addition to brine concentration, another significant factor must have influenced the transformation of layered aluminosilicates, slowing their aggradational transformation. This influence likely involved organic compounds, sorbed by interlayer intervals of labile clay minerals (smectite, corrensite and mixed-layer phases), that prevented the entrance of inorganic cations (potassium, magnesium and other) and increased the resistance of those minerals to transformation in the conditions of a salt-forming basin. Diffractograms of clay minerals of the Hrynivka and Silets-Stupnytsya sites show the presence of sorbed organic compounds (see below).

An increased brine concentration causes aggradational transformation of clay minerals – changes targeted to the structural ordering through the capture of cations and the decrease of molecular volume. This process is clearly supported by the example of transformation of unstable and labile minerals and phases (kaolinite, smectite and mixed-layer phases) that were supplied to Miocene evaporite basins of the Carpathian Foredeep from the continent and through a number of transformations, transformed into illite and chlorite; minerals stable in an evaporite environment. Those two minerals compose the association of clay minerals in the Kalush-Holyn potash deposit.

Potassium enters the interlayer spaces of smectite and mixed-layer phases due to electrostatic forces of attraction of cations to negatively-charged siloxane sheets, where the excess of negative charge is created by Al moving into tetrahedral positions in the place of Si and Al replacing Mg, Fe^{2+} in octahedral positions [81]. Illitization of smectite as a pure phase as well as packages in mixed-layer

 doi:10.20944/preprints202502.1716.v1

phases is through a heterogeneous reaction that is described by the equation [82]:
montmorillonite + K^+ → illite + (Fe^{2+}, Mg^{2+}) + SiO_2.

In evaporitic conditions smectite is magnesium-rich; during its aggradational transformation the entrance of potassium in the mineral structure leads to liberation of silicon and magnesium, which cause the crystallisation of magnesium-rich chlorite and authigenic quartz. The process of illitization of smectite in hypersaline conditions is accompanied by further development of the illite structure. The generally accepted crystallisation order during progressive illitization is as follows:

smectite → I-S, random → I-S, ordered → illite, $1M_d$ → muscovite, $2M_1$ (e.g., [83]). Such transformation is noted during the diagenetic change of smectite at a temperature of ~360 °C [84]. In an evaporitic environment, we infer that, rather than temperature, the main factor is high salinity that caused a further aggradation of illite. This is why micas of $2M_1$ polytype are the only stable minerals among the entire series of aggradational transformation of smectite at progressively higher salinities. Better ordering of the illite structure and its transformation to mica is observed in clay minerals of the Kalush-Holyn potash deposit.

Thin intercalations of tuffs and tuffites occurring in the Kalush-Holyn deposit [85,86] indicate that pyroclastic material was also supplied to the evaporite basin. During the decomposition of volcanic glass, trioctahedral smectite was formed that through chlorite-smectite was finally transformed into trioctahedral chlorite. No intermediate products of this transformation were recorded, though. In clay minerals related to the rock salt occurring in the Sambir zone of the Ukrainian Carpathian Foredeep an excess of mixed-layer phases was observed [56,60] and they are clearly fixed products of decomposition of pyroclastic material. A more complex picture emerges from study of the Tyras gypsum. [57] concluded that the composition of clay minerals in that gypsum does not indicate volcanogenic input into the evaporite basin, possibly because the decomposition of pyroclastic material that leads to the formation of trioctahedral smectite had just begun due to low brine concentration in the basin, this conclusion being supported by an admixture of trioctahedral smectite in the pelitic fraction. However, [87] recorded a bed 5-20 cm thick of bentonite clay that is a local marker of the Badenian gypsum in the region between the Seret and Zbruch rivers.

4.2. Organic Matter Control

Previous research indicated that the low reactivity of clay minerals may be attributed to the presence of organic matter in the samples [88], and that this anomalous lack of evolution (i.e., transformations) of clay minerals is due to specific interactions between organic matter and clay minerals [89].

Clay mineral particles actively sorb organic compounds both onto outer surfaces and in the mineral structure, in interlayer intervals. In the first case, their surface defects and sides perpendicular to the silicate sheets, broken chemical bonds of which actively contribute to sorption of organic ions [90], and to a lesser extent onto cleavage surfaces. Due to the high dispersion of clay particles, the total surface is large and can adsorb a significant amount of organic matter. Organic matter (including scattered and epigenetic) as well as others amorphous materials in diffractograms appears in the form of a halo which looks like a broad hump of low intensity. The position of the amorphous halo (°2Θ) on the diffractograms is correlated with the material of the X-ray tube anode and varies in the d/n range of 0.88-0.225 nm [91]. The halos with maxima of 0.45 and 0.34-0.37 nm characterise the sapropel and aromatic components of organic matter, respectively [92]. The presence of a halo on diffractograms of clay minerals in the field 22–36 °2Θ may be caused by the adsorption of amorphous organic matter onto clay surfaces. Adsorption of organic compounds is characteristic on external surfaces of all types of clay particles, though intercalation of organic compounds into interlayer intervals is typical only for swelling structures. In labile interlayer intervals of clay minerals, organic molecules may be preferentially intercalated from a solution relative to cations of alkaline or alkaline earth elements, and can also replace those cations in these intervals [90,93]. At the same time the crystal lattice of smectite and mixed-layer phases becomes disordered extended along the C axis [94], leading to the appearance of additional low-intensity reflections in the 3–7 °2Θ area

 doi:10.20944/preprints202502.1716.v1

of the diffractograms. Lesser adsorption is characteristic of illite, though only for swelling packages in its structure.

Organic ions or compounds, that in the clay mineral structure occupy exchange positions, are linked by Van der Waals bonds. An additional factor in retaining aliphatic organic compounds is the similarity of the structure of hydrocarbon chains, composed of hydrogen tetrahedra, to certain directed elements in the layered aluminosilicate (clay mineral) sheets, represented by siloxane tetrahedra [95].

The diffraction spectra of clay minerals associated with rock salt of the Carpathian Foredeep Basin are interpreted both in terms of sorption of organic compounds on the surfaces and in the mineral structure. All spectra of the basal reflections of the Badenian rock salt show an increased position of the line of background and halo with numerous lines of low intensity in the area of 22–36 °2Θ. The pelitic fraction of both the Badenian and Eggenburgian rock salt in the area of low angles (4–7 °2Θ) is fixed by a series of reflections, that do not cover the diffraction from the basal planes of the clay structures. These reflections do not change their position in ethylene-glycolated conditions, and a part of them remains on diffractograms after thermal treatment (T = 550 °C) [60].

The possible influence of epigenetic organic matter (bitumen) on the transformation of clay minerals remains controversial, especially as regards the duration of the processes involved. At the stages of sedimentation and early diagenesis, syndepositional, biochemically decomposed organic matter in a brine-saturated deposit in an evaporite basin, adsorbed onto labile clay minerals, became intercalated into the interlayer spaces, hindering the entrance of inorganic cations and slowing their transformation. Epigenetic organic matter got into evaporite deposits considerably later, at the late diagenetic stage. In the Carpathian Foredeep the formation of regional overthrusts created pathways of bitumen migration that are geochemically recorded in the Miocene evaporite deposits of that region (e.g., [96]). Bitumen compounds are undoubtedly adsorbed onto clay minerals; there remains an unresolved question as to how this influenced the transformation of the clay minerals. We commonly assume that in a lithified evaporite succession the transformation of clay minerals continued, although at a slower rate, and intercrystal brines in the deposit provided a supply of cations or organic compounds. That is, epigenetic organic matter also participated in the transformation of clay minerals in the Badenian evaporite deposits.

Organic compounds captured by the structure prevent the entrance of inorganic cations in interlayer intervals. This stopped or slowed the transformation of clay minerals, and increased their resistance to changes in physico-chemical conditions of the environment. In evaporite deposits, as salt concentration increases, the clay minerals transform, ordering their structure and decreasing the number of swelling minerals [59]. The final products of such transformation during the progressive evaporite process are illite and chlorite. Smectite and mixed-layer chlorite-smectite are characteristic only of the initial, sulfate-carbonate stage of evaporation. At the halite stage, only a small content of mixed-layer phases is present, and the main minerals are illite and chlorite. The same is the case for the association of clay minerals in the Eggenburgian rock salt of the Vorotyshcha Suite – this is represented by illite and chlorite with a small content of mixed-layer illite-smectite, rarely (only in two samples out of ten) with an insignificant admixture of mixed-layer chlorite-smectite [55].

4.3. Fresh Water Control During Hypergenesis

Clay minerals of the hypergenesis zone deposits of the Carpathian Foredeep have been studied only rarely: [97] found illite and mixed-layer illite-smectite in the gypsum-clay caprock of Dombrovo Quarry, the Kalush-Holyn deposit, and [98] recorded kaolinite and illite in the gypsum-clay caprock of the Stebnyk deposit.

The hypergene deposits of the Kalush-Holyn potash salt accumulation are exposed in Dombrovo Quarry, where in the gypsum-clay caprock the association of clay minerals contains, in addition to illite and chlorite, also mixed-layer illite-smectite, and in half of the samples additionally kaolinite was found that was not recorded in the evaporite rocks before they suffered the dissolution

 doi:10.20944/preprints202502.1716.v1

by fresh water. Associations of clay minerals above the potash rocks as well as above salt-bearing breccia do not differ (see Table 4).

In the weathering zone of the Kalush-Holyn deposit, fresh, surface waters come into contact with evaporites and dissolve them. A considerable decrease in brine concentration causes degradational transformation of the clay minerals. Our data indicate that the associations of clay minerals of the weathering zone, in addition to illite and chlorite, inherited from evaporite deposits, contain also mixed-layer illite-smectite and kaolinite – minerals that have originated in deposits of the hypergene zone. The appearance of these clay minerals in hypergene deposits is a consequence of transformation (degradation) of clay structures and neoformation when ionic concentrations decrease under the influence of fresh surface waters. Degradational transformation of mica and illite is the reverse process to aggradation and acts to leach potassium from the structure with water molecules penetrating into interlayer spaces. To restore electrostatic equilibrium, Fe and Mg ions migrate into the structure, from octahedral sheets to interlayer intervals, and Al moves from tetrahedral to octahedral positions. Degradation starts from the peripheries of clay particles. As size decreases, specific surface area increases which promotes migration and element liberation. Structural defects accelerate the degradation process [4].

During degradational transformation, mica is completely converted into illite that in interlayer intervals contain partly hydrated potassium ions [84,99]. With continued formation of labile interlayer intervals, mixed-layer illite-smectite appears. Ionic bonds are moderately strong and are difficult to break, which explains the small content of mixed-layer illite-smectite. The capture of potassium by mixed-layer illite-smectite and its transition into illite (aggradational transformation) happens more easily than the reverse process – leaching of potassium and transformation of illite into mixed-layer illite-smectite (degradational transformation). We infer that kaolinite in hypergene deposits of the Kalush-Holyn accumulation is authigenic newly-formed mineral. This is indicated by an absence of clay minerals in the evaporite deposits that could be transformed in kaolinite. Kaolinite forms during the reaction of Al-(hydr)oxides that are released during intense leaching, with silica in weakly acidic conditions (pH ~5), when silica activity is low and the concentration of basic cations is low [68].

Let us consider if such conditions occurred in the gypsum-clay caprock. During dissolution of potash deposits from the lower part of the gypsum-clay caprock, conditions in the brine were weakly acidic, as during sedimentation of the potash deposits. Thus, in the precipitation field of K-Mg salts, pH values decreased to 5.7 [69,72]. Similar results were obtained in a fluid inclusion study of Miocene evaporites of the Carpathian Foredeep [100]: pH ranged from 4.5 to 6.6, averaging 5.6. Kaolinite formed only in the lower part of the gypsum-clay caprock; in its middle and upper parts kaolinite appears, and it increases upwards. Its presence indicates that conditions existed here that have favoured its preservation. Oxides and hydroxides of aluminium and silicon, necessary for the crystallisation of kaolinite, were released during the degradation of illite to mixed-layer illite-smectite. All this indicates that during the formation of the gypsum-clay caprock there existed the physico-chemical conditions necessary for kaolinite crystallisation.

4.4. Burial Depth and Geothermal Regime Control

The Eggenburgian and Badenian evaporites studied occur at depths of 600–700, rarely 1500 m [23]. The thermobarimetric analysis of fluid inclusions in the Miocene evaporite deposits of the Ukrainian Carpathian Foredeep indicates that the temperature at the diagenesis stage in the halite of the salt-bearing breccia was 35–40 °C and 60–80 and even 110 °C in the potash facies [101,102]. However, those higher values are explained by [102] as due to various exothermic reactions related to evaporite minerals such as the conversion of metastable mineral phases and minerals into stable ones or radioactive decay of potassium.

Surface heat flow within the Ukrainian Carpathian fold-thrust belt and adjacent East European platform varies from 35 to 130 mW/m^2, with lower values dominating the East European platform

 doi:10.20944/preprints202502.1716.v1

[103]. Heat flow has not been elevated in the nappes adjacent to the East European platform since the Oligocene [104].

A geothermal gradient of ~37 °C/km is assumed as a maximum value for the Ukrainian Carpathians (including the Carpathian Foredeep) [105]. Based on analysis of fluid inclusions, [106], and references therein proposed slightly higher (up to 3-5° C/km) gradient estimates than those proposed by [104].

[105] concluded that the outermost and innermost Carpathian thrust sheets were heated to less than 60 °C and less than ~120 °C, respectively; the heating depended entirely on burial, and the cooling occurred in two main phases (15-30 °C/m.y. between ca. 12 and ca. 5 Ma, 3-6 °C/m.y. from ca. 5 Ma to the present), and was induced by exhumation. The pressure and temperature in the Miocene evaporite deposits of the Ukrainian Carpathian Foredeep did not reach values characteristic of the late diagenesis and anchizone, and thus the transformation processes of clay minerals in those deposits are controlled by other causes than pressure and temperature.

5. Conclusions

Brine concentration control is the most important factor determining the clay mineral transformation of marine evaporite sequences. Clay minerals associated with the gypsum, halite and potash facies of the Miocene evaporite formations of the Ukrainian Carpathian Foredeep reflect the increased concentration of brines that promoted the aggradational transformation of labile clay minerals into illite and chlorite that are stable in hypersaline conditions. Further ordering of the structure led to transformation of illite into mica.

Brine concentration decrease (inflow of fresh water) led to slowing of transformation of clay minerals, and as a result in the Badenian gypsum and rock salt, an association untypical for the gypsum and halite facies originated: only a small content of mixed-layer phases in the gypsum facies and, in the halite facies, a considerable amount of labile swelling minerals that did not transform into illite and chlorite.

Organic matter control is another important (but local) factor of transformation of clay minerals of the Miocene evaporites. Organic compounds, sorbed by labile clay minerals and mixed-layer phases, prevented the entrance of inorganic cations into their interlayer intervals, suspending or delaying their aggradational transformation. A large number of labile clay minerals in the Badenian rock salt (smectite, corrensite and mixed-layer phases) are still present owing to organic compounds captured by the structures of these minerals.

Clay minerals of the Badenian rock salt interacted with epigenetic organic matter entering the Miocene evaporite deposits during the origin of regional overthrusts in the Carpathian Foredeep that created pathways of bitumen migration.

Fresh water control in hypergene conditions during the dissolution of evaporite deposits by fresh surface waters is the common factor determining the clay minerals' degradational transformation that involves partial leaching of potassium from the interlayer spaces of illite and the formation of illite-smectite (degradational transformation) and kaolinite (neoformation) in the gypsum-clay caprock of Dombrovo Quarry (the Kalush-Holyn potash deposit).

Author Contributions: Conceptualization: Y.Y., S.H., T.P.; methodology: Y.Y., S.H.; investigation: Y.Y., S.H.; data curation: Y.Y., S.H.; formal analysis: Y.Y., S.H., T.P.; visualization: Y.Y., S.H., T.P.; writing—original draft preparation: Y.Y., S.H.; writing—review and editing: T.P., Y.Y., S.H. All authors have read and agreed to the published version of the manuscript.

Funding: This research was supported by the National Academy of Sciences of Ukraine statutory funds.

Data Availability Statement: Research data are available on request.

Acknowledgments: We are very grateful to the late V.M. Kovalevych for consultations and general guidance during the initial stage of this research (2004-2013). We also thank J. Zalasiewicz for his helpful suggestions on the manuscript, and to the journal referees for their comments.

Conflicts of Interest: The authors declare no conflict of interest.

 doi:10.20944/preprints202502.1716.v1

References

1. Millot, G. *Geology of Clays: Weathering, Sedimentology, Geochemistry*; Springer: New York; Berlin, 1970; pp. 429.
2. Eberl, D.D.; Farmer, V.C.; Barrer, R.M. Clay Mineral Formation and Transformation in Rocks and Soils [and Discussion]. *Phil. Transact. Royal Soc. Lond. Series A, Math. Phys. Sci.* **1984**, *311*, 241-257.
3. Lucas, J. La transformation des minéraux argileux dans la sédimentation. Etudes sur les argiles du Trias. *Mém. Serv. carte géol. d'Alsace et de Lorraine* **1962**, *23*, 1-202.
4. Millot, G.; Lucas, J.; Paquet, H. Evolution géochimique par dégradation et agradation des minéraux argileux dans l'hydrosphère. *Geol. Rd.* **1966**, *55*, 1–20.
5. Dunoyer de Segonzac, G. The transformation of clay minerals during diagenesis and low-grade metamorphism: a review. *Sediment.* **1970**, *15*, 281–346.
6. Lanson, B.; Sakharov, B.A.; Claret, F.; Drits, V.A. Diagenetic smectite-to-illite transition in clay-rich sediments: A reappraisal of X-ray diffraction results using the multi-specimen method. *Am. Jour. Sci.* **2009**, *309*, 476–516.
7. Bodine, M.W., Jr. Trioctahedral Clay Mineral Assemblages in Paleozoic Marine Evaporite Rocks. In *Sixth International Symposium on Salt*; Salt Institute: Alexandria, VA, USA, 1985; Volume 1, pp. 267–284.
8. Warren, J.K. *Evaporites: A Compendium*; Springer: Berlin/Heidelberg, Germany, 2016; pp. 1854.
9. Kossovskaya, A.G.; Drits, V.A. Kristallokhimiya dioktaedricheskikh slyud, khloritov i korrensitov kak indikatorov geologicheskikh obstanovok. In *Problemy Litologii i Geokhimii Osadochnykh Porod i Rud*; Nauka: Moskva, USSR, 1975; pp. 60–69. (In Russian)
10. Sokolova, T.N. Autigennoe silikatnoe mineraloobrazovanie raznykh stadiy osolonennya. *Tr. GIN* **1982**, *361*, 1–164. (In Russian)
11. Bilonizhka, P.M. The clay minerals as indicators of salt deposition conditions in Precarpathian Foredeep. *Geol. Geochem. Comb. Min.* **1992**, *78*, 95–102. (In Ukrainian with English abstract).
12. Bilonizhka, P.M. The transformation of terrigenous clay minerals in the saliferous process. *Miner. Zb.* ***1992***, *45* (2), 51–56. (In Ukrainian with English abstract)
13. Calvo, J.P.; Blanc-Valleron, M.M.; Rodriguez Arandia, J.P.; Rouchy, J.M.; Sanz, M.E. Authigenic clay minerals in continental evaporitic environments. *IAS Spec. Publ.* **1999**, *27*, 129–151.
14. Turner, C.E.; Fishman, N.S. Jurassic Lake T'oo'dichi: a large alkaline, saline lake, Morison Formation, eastern Colorado Plateau. *Geol. Soc. Amer. Bull.* **1991**, *103*, 538–558.
15. Uhlík, P.; Honty, M.; Šucha, V.; Franců, J.; Biroň, A.; Clauer, N.; Hanzelyová, Z.; Majzlan, J. Influence of salt-bearing environment to illitization. In *Proceedings of the XVII Congress of CBGA*, Bratislava (CD-ROM). (*Geol. Carp.* **53**), 2002.
16. Honty, M.; Uhlík, P.; Šucha, V.; Čaplovičova, M.; Franců, J.; Clauer, N.; Biroň, A. Smectite-to-illite alteration in salt-bearing bentonites (East Slovak Basin). *Clay Clay Miner.* **2004**, *52*, 533–551.
17. Bilonizhka, P.; Iaremchuk, Ia.; Hryniv, S.; Vovnyuk, S. Clay minerals of Miocene evaporites of the Carpathian Region, Ukraine. *Biul. Państw. Inst. Geol.* ***2012***, *449*, 137–146.
18. Velde, B. *Clay Minerals. A physico-chemical explanation of their occurrence*; Elsevier: Amsterdam, 1985, pp. 427.
19. Oszczypko, N.; Krzywiec, P.; Popadyuk, I.; Peryt, T. Carpathian Foredeep Basin (Poland and Ukraine): Its sedimentary, structural, and geodynamic evolution. *AAPG Mem.* **2006**, *84*, 293–350.
20. Oszczypko, N.; Uchman, A.; Bubniak, I. The Dobrotiv Formation (Miocene) in the Boryslav-Pokuttya and Sambir nappes of the Ukrainian Carpathians: a record of sedimentary environmental change in the development of the Carpathian Foredeep Basin. *Geol. Quart.* **2014**, *58*, 393–408.
21. Hnylko, O.M. Tectonic zoning of the Carpathians in terms of the terrane tectonics Article 2. The Flysch Carpathian – ancient accretionary prism. *Geodyn.* **2012**, *12*, 67–78. (In Ukrainian with English summary)
22. Peryt, T.M. The beginning, development and termination of the Middle Miocene Badenian salinity crisis in Central Paratethys. *Sed. Geol*. **2006**, *188–189*, 379–396.
23. Rudko, H.I.; Petryshyn, V.Yu. *Soliani resursy Peredkarpattia ta perspektyvy yikh vykorystannia*; Bukrek: Kyiv, Chernivtsi, 2017. (In Ukrainian)

 doi:10.20944/preprints202502.1716.v1

24. Andreyeva-Grigorovich, A.S.; Oszczypko, N.; Ślączka, A.; Oszczypko-Clowes, M.; Savitskaya, N.; Trofimovicz, N. New data on the stratigraphy of the folded Miocene Zone at the front of the Ukrainian Outer Carpathians. *Acta Geol. Pol.* **2008**, *58*, 325–353.
25. Vashchenko, V.O.; Hnylko, O.M. About stratigraphy and sedimentary features of the Neogene molasse of the Boryslav-Pokuttya and Sambir Nappes of the Ukrainian Fore-Carpathians. *Heol. Heokh. Hor. Kop.* **2003**, (1), 87-101. (in Ukrainian with English summary)
26. Vashchenko, V.O.; Hnylko, O.M. About stratigraphy of the salt-bearing molasse of the Ukrainian Fore-Carpathians *Zbirn. Nauk. Prats UkrDGRI* **2013**, *2*, 71–77. (in Ukrainian with English summary)
27. Piller, W.E.; Harzhauser, M.; Mandic, O. Miocene Central Paratethys stratigraphy – current status and future directions. *Stratigraphy* **2007**, *4*, 151–168.
28. Vyalov, O.S. *Stratigrafiya neogenovykh molass Predkarpatskogo progiba*. Naukova Dumka: Kiev, 1965, pp. 192. (In Russian)
29. Dzhinoridze, N.M. Tertiary potassium basins. In V.I. Raievskiy & M.P. Fiveg (eds), *Deposits of potassium salts of the USSR*; Nedra: Leningrad, USSR, 1973; 183-234. (In Russian)
30. Dzhinoridze, N.M. Karpatskiy kalienosnyy region. In *Zakonomernosti Razmeshchenia i Kriterii Poiskov Kaliynykh Soley SSSR*; Izdatelstvo "Mecniereba": Tbilisi, USSR, 1980; p. 73-159. (In Russian)
31. Koriń, S.S. Geology of the Miocene salt-bearing formations of the Ukrainian Fore-Carpathians). *Prz. Geol.* **1994**, *42*, 744–747. (In Polish)
32. Petryczenko, O.I.; Panow, G.M.; Peryt, T.M.; Srebrodolski, I.M.; Pobereżski, A.W.; Kowalewicz, W.M. Outline of the Miocene evaporite formations of the Ukrainian part of the Carpathian Foredeep. *Prz. Geol.* **1994**, *42*, 734-737.
33. Peryt, T.M.; Hryniv, S. On strontium isotope composition of Miocene potash evaporites in the Ukrainian Carpathian Foredeep. *Heol. Heokh. Hor. Kop.* **2011**, *156-157*, 81-94.
34. Vashchenko, V.O.; Turchynova, S.M.; Turchynov, I.I.; Polikha, G.G. *Derzhavna geologichna karta Ukrainy 1:200 000. Karpatska seriya. Arkush M-35-XXV (Ivano-Frankivsk). Poyasnyu valna zapiska*. UkrDGI, Kyiv, 2007. (In Ukrainian)
35. Andreyeva-Grigorovich, A.S.; Vashchenko, V.O.; Hnylko, O.M.; Trofimovich, N.A. Stratigraphy of Neogene deposits of the Ukrainian Carpathians and Carpathian Foreland. *Tekt. Stratyhr*. **2011**, *28*, 67–77. (In Ukrainian with English summary)
36. Hnylko, O. Olistostromes in the Miocene salt-bearing folded deposits at the front of the Ukrainian Carpathian orogen. *Geol. Quart*. **2014**, *58*, 381–392.
37. Korin, S.S. Tektonicheskiye usloviya formirovaniya struktury kaliynykh mestorozhdeniy v Boryslavsko-Pokutskom pokrove. *Otech. Geol.* **1992**, no. 12, 20-26. (in Russian)
38. Peryt, T.M.; Kovalevich, V.M. Association of redeposited salt breccias and potash evaporites in the Lower Miocene of Stebnyk (Carpathian Foredeep, West Ukraine). *J. Sediment. Res.* **1997**, *67*, 913–922.
39. Korenevskiy, S.M.; Donchenko K.B. Geologiya i usloviya formirovaniya kaliynykh otlozheniy Sovetskogo Predkarpatia. *Tr. VSEGEI, N.S.* **1963**, *99*, 3–153. (In Russian)
40. Czapowski, G.; Bukowski, K.; Tomassi-Morawiec, H.; Toboła, T. Geochemistry and mineralogy of Miocene Zuber rocks in the Carpathian Foredeep (southern Poland). *Prz. Solny* **2023**, *17*, 39-50.
41. Shestopalov, M.; Liutyi, H.; Sanina, I. Suchasni pidkhody do hidroheolohichnoho raionuvannia Ukrainy. *Mineralni resursy Ukrainy* ***2019***, *2*, 3–12. (In Ukrainian)
42. Wójtowicz, A.; Hryniv, S.P.; Peryt, T.M.; Bubniak, A.; Bubniak, I.; Bilonizhka, P.M. K-Ar dating of the Miocene potash salts of the Carpathian Foredeep (West Ukraine): application to dating of tectonic events. *Geol. Carp.* **2003**, *54*, 243–249.
43. de Leeuw, A.; Bukowski, K.; Krijgsman, W.; Kuiper, K.F. Age of the Badenian salinity crisis; impact of Miocene climate variability on the circum-Mediterranean region. *Geology* **2010**, *38*, 715–718.
44. Peryt, T.M. Sedimentology of Badenian (middle Miocene) gypsum in eastern Galicia, Podolia and Bukovina (West Ukraine). *Sediment.* **1996**, *43*, 571–588.
45. Peryt, T.M. Gypsum facies transitions in basin-marginal evaporites: middle Miocene (Badenian) of West Ukraine. *Sediment.* **2001**, *48*, 1103–1119.

 doi:10.20944/preprints202502.1716.v1

46. Bąbel, M. Badenian evaporite basin of the northern Carpathian Foredeep as a drawdown salina basin *Acta Geol. Pol.* **2004**, *54*, 317-337.
47. Bąbel, M. Selenite-gypsum microbialite facies and sedimentary evolution of the Badenian evaporitic basin of the northern Carpathian Foredeep. *Acta Geol. Pol.* **2005**, *55*, 187-210.
48. Peryt, T.M. Palaeogeographical zonation of gypsum facies: Middle Miocene Badenian of Central Paratethys (Carpathian Foredeep in Europe). *J. Palaeogeogr.* **2013**, *2*, 225-237.
49. Kasprzyk, A.; Orti, F. Paleogeographic and Burial Controls on Anhydrite Genesis: The Badenian Basin in the Carpthian Foredeep (Southern Poland, Western Ukraine). *Sediment.* **1998**, *45*, 889-907.
50. Hryniv, S.P.; Dolishniy, B.V.; Khmelevska, O.V.; Poberezhskyy, A.V.; Vovnyuk, S.V. Evaporites of Ukraine: a review. *Geol. Soc. Spec. Publ.* **2007**, *285*, 309–334.
51. Galamay, A.R.; Bukowski, K.; Zinchuk, I.M.; Meng, F. The Temperature of Halite Crystallization in the Badenian Saline Basins, in the Context of Paleoclimate Reconstruction of the Carpathian Area. *Minerals* **2021**, *11*, 831.
52. Bukowski, K. *Badenian Saline Sedimentation between Rybnik and Dębica Based on Geochemical, Isotopic, and Radiometric Research*; Dissertation Monographs 236; AGH: Kraków, Poland, 2011; pp. 184. (In Polish with English summary)
53. Palcu, D.V.; Mariş, I.; de Leeuw, A.; Melinte-Dobrinescu, M.; Anton, E.; Frunzescu, D.; Popov, S.; Stoica, M.; Jovane, L.; Krijgsman, W. The legacy of the Tethys Ocean: Anoxic seas, evaporitic basins, and megalakes in the Cenozoic of Central Europe. *Earth-Sci. Rev.* **2023**, *246*, 104594,
54. Oliiovych, O.; Iaremchuk, Ia.; Hryniv, S. Hlyny halohennykh vidkladiv i kory zvitriuvannia Kalush-Holynskoho rodovyshcha kaliinykh solei (miotsen, Peredkarpattia). *Miner. Zb.* **2004**, *54* (2), 214–223. (In Ukrainian)
55. Iaremchuk, I.; Hryniv, S. Mineral'nyy sklad hlyn kam"yanoyi soli miotsenovykh evaporytiv Karpat·s'koho rehionu Ukrayiny. In *Suchasni Problemy Litolohiyi i Mineraheniyi Osadovykh Baseyniv Ukrayiny ta Sumizhnykh Terytoriy*; IHN Ukrayiny: Kyiv, Ukraine, 2008; p. 209–215. (In Ukrainian)
56. Iaremchuk, Ia.; Galamay, A. Mineral composition of the water insoluble residue from rock salt Hrynivka area of the Carpathian Foredeep. *Heol. Heokh. Hor. Kop.* **2009**, *146*, 79–90. (In Ukrainian with English abstract)
57. Iaremchuk, Ia., Poberezhsky, A. Clay mineral composition of Badenian gypsum of the Dnister-River region. *Miner. Zb.* **2009**, *59*, 116–127. (In Ukrainian with English summary)
58. Iaremchuk, Ia. *Clay minerals of Phanerozoic evaporates and their dependence upon brine concentration stage and seawater chemical type*. Avtoref. Dis. Kand. Heol. Nauk, Lviv 2010, pp. 24. (In Ukrainian with English summary)
59. Iaremchuk, Ia. Dependence of clay mineral associations of the Neogene evaporates from the Carpathian region upon the salt brines concentration in salt-producing basins. *Heol. Heokh. Hor. Kop.* **2012**, *160–161*, 119–130. (In Ukrainian with English summary)
60. Iaremchuk, Ia.; Hryniv, S. Organic matter effect on composition and genesis of clay minerals of rock salt deposits of the Carpathian Foredeep. *Heol. Heokh. Hor. Kop.* **2013**, *162-263*, 60-70. (In Ukrainian with English abstract)
61. **Hryniv, S.; Yaremchuk, Y.; Radkovets, N.** The influence of marine and continental waters on the clay minerals transformation processes of evaporite deposits (on the example of the Kalush-Holin' deposit, Carpathian Foredeep). *Geol. Geochem. Comb. Min.* **2023**, *191–192*, 122–134. (In Ukrainian with English summary)
62. Moore, D.M.; Reynolds Jr., R.C. *X-ray Diffraction and the Identification and Analysis of Clay Minerals*; Oxford University Press: New York, 1997; pp. 376.
63. Brown, G.; Brindley, G.W. X-Ray Diffraction Procedures for Clay Mineral Identification. *Mineralogical Society Monograph* **1980**, *5*, 305-356.
64. Bish, D.L.; Duffy, C.J. Thermometric analysis of minerals. *Clay Minerals Society Workshop Lectures* **1990**, *3*, 96-157.
65. Drits, V.A.; Kossovskaya, A.G. *Glinistyye mineraly: smektity, smeshanosloynyye obrazovaniya*; Nauka: Moskva, 1990; pp. 214. (In Russian)

 doi:10.20944/preprints202502.1716.v1

66. Bilonizhka, P.M. Pryroda mizhsharovoi vody v hidrosliudakh. *Miner. Zb.* ***2001***, *51*(1), 142–148. (In Ukrainian)
67. *Drits,* V.A.; *Sakharov,* B.A. *X-ray structure analysis of interstratified minerals*; Nauka: Moskva, 1976; pp. 256. (In Russian)
68. Galán, E. Genesis of Clay Minerals. In F. Bergaya, B.K.G. Theng & G. Lagaly (Eds.), *Developments in Clay Science: Vol. 1. Handbook of Clay Science* (Ch. 14, pp. 1129–1162). Amsterdam: Elsevier, 2006.
69. Bąbel, M.; Schreiber, B.C. Geochemistry of Evaporites and Evolution of Seawater. *Treatise Geochem.* **2014**, *9*, 483–560.
70. Yaremchuk, Y.; Hryniv, S.; Peryt, T.; Vovnyuk, S.; Meng, F. Controls on Associations of Clay Minerals in Phanerozoic Evaporite Formations: An Overview. *Minerals* **2020**, *10* (11), 974.
71. Lanson, B.; Beaufort, D.; Berger, G.; Bauer, A.; Cassagnabere, A.; Meunier A. Authigenic kaolin and illitic minerals during burial diagenesis of sandstones: a review. *Clay Miner.* **2002**, *37*, 1–22.
72. McCaffrey, M.A.; Lazar, B.; Holland, H.D. The evaporation path of seawater and the coprecipitation of Br and K with halite. *J. Sediment. Res.* **1987**, *57*, 928–937.
73. Dopieralska, J., Belka, Z., Zieliński, M., Górka, M., Poberezhskyy, A., Stupka, O., Walczak, A., Wysocka, A., 2024. Neodymium and strontium isotopes track the origin of parent brines of primary gypsum deposits (Miocene, Fore-Carpathian Basin). *Chem. Geol.* **2024**, *648*, 121963
74. Petrichenko, O.I.; Peryt, T.M.; Poberegsky, A.V. Pecularities of gypsum sedimentation in the Middle Miocene Badenian evaporite basin of Carpathian Foredeep. *Slovak Geol. Mag.* **1997**, *3*, 91–104.
75. Kovalevich, V.M.; Petrichenko, O. I. Chemical composition of brines in Miocene evaporite basins of Carpathian region. *Slovak Geol. Mag.* **1997**, *3*, 173–180.
76. Peryt, T.M.; Szaran, J.; Jasionowski, M.; Halas, S.; Peryt, D.; Poberezhskyy, A.; Karoli, S.; Wójtowicz, A. S and O isotope composition of the Badenian (Middle Miocene) sulphates in the Carpathian Foredeep. *Geol. Carp.* **2002**, *53*, 391–398.
77. Peryt, T.M.; Hryniv, S.P.; Anczkiewicz, R. Strontium isotope composition of Badenian (Middle Miocene) Ca-sulphate deposits in West Ukraine: a preliminary study. *Geol. Quart.* **2010**, *54*, 465–476.
78. Galamay, A.R. Physico-chemical conditions of the formation of the Badenian salt deposits of the Ukrainian Forecarpathians (Grynivka area). *Heol. Heokh. Hor. Kop.* **2010**, (2), 64–77. (In Ukrainian with English summary)
79. Galamay, A.R. Influence of continental run-off on the composition of marine brines of Badenian salt basin central part (Ukrainian Carpathian Foredeep). *Miner. Zb.* **2012**, *62*, 228–235. (In Ukrainian with English summary)
80. Zhao, Y.; Wei, H.-Z.; Liu, X.; Wang, Y.-J.; Jiang, S.-Y.; Eastoe, C.F.; Peryt, T.M. Isotope evidence for multiple sources of B and Cl in Middle Miocene (Badenian) evaporites, Carpathian Mountains. *Appl. Geochem.* **2021**, *124*, 104819.
81. Środoń, J. Illite group clay minerals. In G.V. Middleton, M.J. Church, M. Coniglio, L.A. Hardie & F.J. Longstaffe (Eds.), *Encyclopedia of Sediments and Sedimentary Rocks* (p. 115). Dordrecht: Springer, 1978.
82. Meunier, A. *Clays*. Springer: Berlin Heidelberg, 2005; 472 pp.
83. Zhao, G.; Peacor, D.R.; McDowell, S.D. "Retrograde diagenesis" of clay minerals in the Precambrian Freda Sandstone, Wisconsin. *Clays Clay Miner.* **1999**, *47*, 119–130.91.
84. Rosenberg, P.E. The nature, formation, and stability of end-member illite: a hypothesis. *Am. Miner.* **2002**, *87*, 103–107.
85. Korenevskiy, S.M. Miotsenovyye vulkanicheskiye tufy Predkarpatia. *Tr. VNIIGalurgii* **1954**, *29*, 176–196. (In Russian)
86. Dzhinoridze, N.M.; Rogova, M.S.; Telegin, V.P. Vulkanogennyye porody Kalush-Golynskogo mestorozhdeniya kaliynykh soley. *Tr. VNIIGalurgii* **1974**, *71*, 36–56. (In Russian)
87. Turchinov, I.I. The Badenian (Middle Miocene) gypsum section in Kryvche (Podolia, West Ukraine). *Biul. Państw. Inst. Geol.* **1999**, *387*, 70–74.
88. Claret, F.; Bauer, A.; Schäfer, T.; Griffault, L.; Lanson, B. Experimental investigation of the interaction of clays with high pH solutions: A case study from the Callovo-Oxfordian formation, Meuse-Haute Marne underground laboratory (France). *Clays Clay Miner.* **2002**, *50*, 633-646.

 doi:10.20944/preprints202502.1716.v1

89. Claret, F.; Sakharov, B.A.; Drits, V.A.; Velde, B.; Meunier, A.; Griffault, L.; Lanson, B. Clay minerals in the Meuse-Haute Marne underground laboratory (France): possible influence of organic matter on clay mineral evolution. *Clays Clay Miner.* **2004**, *52*, 515–532.
90. Klubova, T.T. *Glinistye mineraly i ikh rol v genezise, migratsii i akkumulatsii nefti*; Nedra: Moskva, 1973, pp. 255. (In Russian)
91. Rowe, M.C., Brewer, B.J. AMORPH: A statistical program for characterizing amorphous materials by X-ray diffraction. *Computers and Geosciences* **2018**, *230*, 21-31.
92. Korchagina, Yu.I.; Chetverikova, O.P. Metody issledovaniya rasseyannogo organicheskogo veshchestva osadochnych porod; Nedra: Moskva, USSR, 1976; pp. 229. (In Russian)
93. Whitehouse, U.W.; McCarter, R.S. Diagenetic modification of clay mineral types in artifical sea water. *Clays Clay Miner.* **1958**, *5*, 81–119.
94. Grim, R.E. *Clay Mineralogy*; McGraw-Hill Book Company: New York, NY, USA, 1969; 422 pp.
95. Moore, D.M.; Reynolds Jr., R.C. *X-ray Diffraction and the Identification and Analysis of Clay Minerals*; Oxford University Press: New York, 1997; 376 pp.
96. Więcław, D.; Lytvyniuk, S.; Kovalevych, V.; Peryt, T.M. Fluid inclusions in halite and bitumens in rock salt from Miocene evaporites in the Ukrainian Fore-Carpathian region: evidence for hydrocarbon accumulations in the underlying strata. *Prz. Geol.* **2008**, *56*, 837–841. (In Polish with English summary)
97. Semchuk, Ya.M. *Naukovi ta metodychni osnovy okhorony heolohichnoho seredovyshcha v raionakh rozrobky kaliinykh rodovyshch (na prykladi Peredkarpattia)*; Vasyl Stefanyk Precarpathian National University: Ivano-Frankivsk, 1995. (In Ukrainian)
98. Lipnitskiy, V.K. Litologicheskiye osobennosti i solevoy kompleks chetvertichnykh otlozheniy i porod gipsovo-glinistoy shlyapy Stebnikskogo mestorozhdeniya kaliynykh soley; In *Materialy po gidrogeologii i geologicheskoy roli podzemnykh vod*; Izdatelstvo Leningradskogo universiteta: Leningrad, USSR, 1971; pp. 98–108. (In Russian)
99. Środoń, J.; Elsass, F.; McHardy, W.J.; Morgan, D.J. Chemistry of illite-smectite inferred from TEM measurements of fundamental particles. *Clay Miner.* **1992**, *27*, 137–158
100. Petrichenko, O.Yo. *Fiziko-khimicheskiye usloviya osadkoobrazovaniya v drevnikh solerodnykh basseynakh*; Naukova Dumka: Kiev, 1988, pp. 128. (In Russian)
101. Kovalevich, V.M. *Fiziko-khimicheskie uslovia formirovania soley Stebnikskogo kaliynogo mestorozhdenia*; Naukova Dumka: Kiev, 1978, pp. 100. (In Russian).
102. Petrichenko, O.I. *Epigenez evaporitov*; Naukova Dumka: Kiev, 1989, pp. 64. (In Russian)
103. Kutas, R.I. Heat flow and geothermal crustal model of the Ukrainian Carpathians. *Geophys. J.* **2014**, *6*, 3-25.
104. Kotarba, M.J.; Koltun, Y.V. The origin and habitat of hydrocarbons of the Polish and Ukrainian parts of the Carpathian Province. *Am. Ass. Petrol. Geol. Mem.* **2006**, *84*, 395-442.
105. Andreucci, B.; Castelluccio, A.; Corrado, S.; Jankowski, L.; Mazzoli, S.; Szaniawski, R.; Zattin, M. Interplay between the thermal evolution of an orogenic wedge and its retro-wedge basin: An example from the Ukrainian Carpathians. *Geol. Soc. Amer. Bull.* **2015**, *127*, 410–427.
106. Vityk, M.O.; Bodnar, R.J.; Dudok, I.V. Fluid inclusions in "Marmarosh Diamonds": Evidence for tectonic history of the Folded Carpathian Mountains, Ukraine. *Tectonophysics* **1996**, *255*, 163–174.